GEOLOGIC MAP OF THE HEADQUARTERS 30 x 60 MINUTE QUADRANGLE, IDAHO

Reed S. Lewis, Russell F. Burmester, Mark D. McFaddan, John D. Kauffman,
P. Ted Doughty, William L. Oakley, and Thomas P. Frost
2007

INTRODUCTION

Geology depicted on this 1:100,000-scale Headquarters 30' x 60' quadrangle map is based on compilation of previous mapping, extensive fieldwork in 2001, and minor follow up in 2002-2006. The areal coverage of the sources used to prepare this map is shown on Figures 1 and 2. The principal sources were 1990 mapping by the Idaho Geological Survey (Lewis and others, 1992a), 1:48,000-scale maps of Hietanen (1962, 1963a, 1963b, and 1968), and 1:24,000-scale mapping by Childs (1982) in the Elizabeth Lake and Junction Mountain 7.5' quadrangles. This Digital Web Map is a preliminary report that has not been editorially reviewed.

This geologic map was funded in part by the U.S. Geological Survey National Cooperative Geologic Mapping Program, USGS Award No. 01HQAG0047.

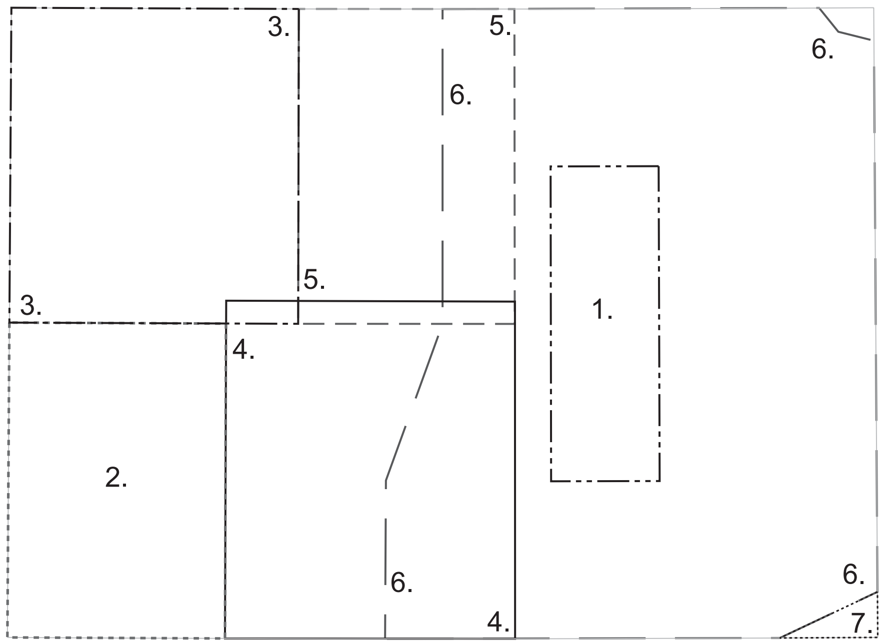

1. Childs, 1982
2. Heitanen, 1962 (Plate 2)
3. Heitanen, 1963a (Plate1)
4. Heitanen, 1963b (Plate1)
5. Heitanen, 1968 (Plate1)
6. Lewis and others, 1992a
7. Lewis and others, 1992b

Figure 1. Index to primary map sources in the Headquarters quadrangle.

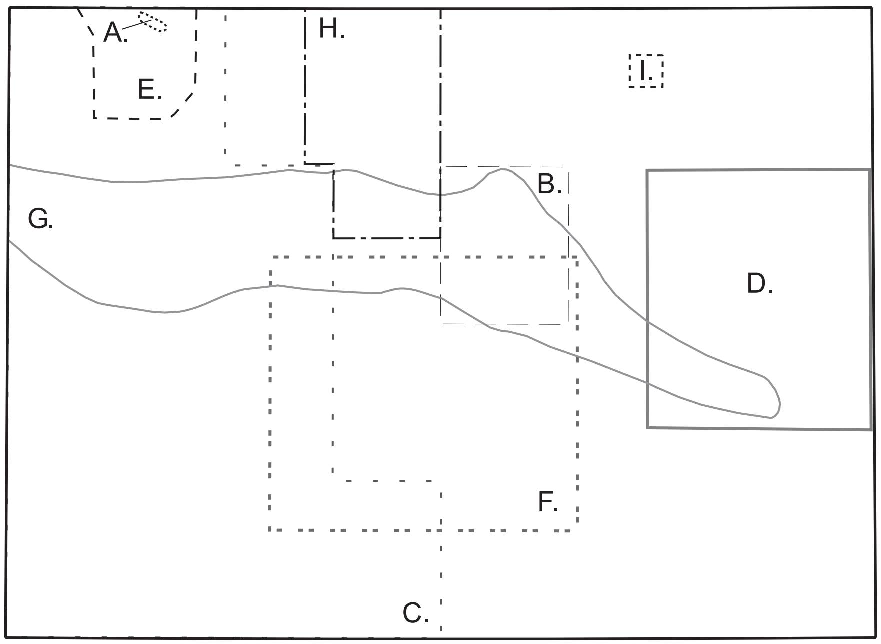

A. Abbott and Prater, 1954
B. Hutchison, 1981
C. M.D. Jenks, unpublished parent material maps of Potlatch Corporation land holdings, 1998
D. R.E. Kell, unpublished geologic map, 1990
E. Nord,1973
F. Reynolds, 1991
G. C.K. Seyfert, unpublished geologic mapping, 1990
H. Standish, 1973
I. Stryhas, 1985b

Figure 2. Index to secondary map sources in the Headquarters quadrangle.

DESCRIPTION OF ROCK UNITS

Intrusive rocks are classified according to IUGS nomenclature using normalized values of modal quartz (Q), alkali feldspar (A) and plagioclase (P) on a Ternary diagram (Streckeisen, 1976). Mineral modifiers are listed in increasing order of abundance for both igneous and metamorphic rocks. Lithologies in mixed units are presented in order of decreasing abundance. Grain size classification of unconsolidated and consolidated sediment is based on the Wentworth scale (Wentworth, 1922).

YOUNG SURFICIAL DEPOSITS

Qal Alluvial deposits (Holocene)—Stream deposits in modern drainages. Primarily channel and flood- plain deposits, but includes local slope-wash and debris-flow deposits from canyon slopes. Most alluvium is composed of laterally discontinuous beds of pebbles, cobbles, sand, and silt.

Qls Landslide deposits (Pleistocene and Holocene)—Poorly sorted and poorly stratified angular cobbles and boulders mixed with silt and clay. Typically associated with sedimentary beds within and basal to flows of Columbia River basalt. The largest landslides occur where valley incision has exposed sedimentary interbeds to steep topography. Also abundant where Paleoproterozoic anorthosite (*Xan*) is exposed. The landslides range from relatively stable features of Pleistocene age to ones that have been active within the past few years.

Qg Glacial deposits (Pleistocene)—Poorly sorted till present in upper parts of high mountain drainages. Locally overlain by more recent coarse debris shed from steep side drainages. Also present, but not mapped, in the headwaters of Sawtooth Creek within the Mallard-Larkins Primitive area near the center of the northern map boundary.

OLDER SEDIMENTS AND SAPROLITE

Ts Sediment, undivided (Miocene and Oligocene?)—Unconsolidated, poorly sorted, fluvial sediment. Includes beds of boulder and cobble gravel, sand, and clay. Typically deeply weathered. Gold-bearing northeast of Pierce near the western end of the southern map boundary and near Independence Creek near the center of the eastern part of the map. Some may be as old as Oligocene; others may be distal high-level equivalents of the Miocene Latah Formation.

Tsap Saprolite (Miocene and Oligocene?)—Clayey residuum weathered in place from parent rock. Shown as pattern on parent rock. Map distribution determined in part from analysis of slope; areas with low slope (not including modern floodplains) typically have well-developed saprolite. Best developed (and preserved) in the southwest part of area. Reflects warmer and wetter Miocene (and older?) climates.

Latah Formation

Tls Latah Formation sediment (Miocene)—Sequences of clay, silt, sand, and minor gravel adjacent to or overlying the Columbia River Basalt Group.

Tli Latah Formation interbed (Miocene)—Sand, silt, clay, and minor amounts of gravel in interbeds between flows of Columbia River Basalt Group. Includes sediments between basement rocks and basalt. Commonly erodes forming benches of slumped sediment and basalt mapped as *Qls*. Only one small unslumped area mapped along Cow Creek near the southwest corner of the map.

COLUMBIA RIVER BASALT GROUP

The stratigraphic nomenclature for the Columbia River Basalt Group follows that of Swanson and others (1979a, 1979b) and Camp (1981). In Idaho, the Columbia River Basalt Group is divided into four formations. From oldest to youngest, these are the Imnaha Basalt, Grande Ronde Basalt, Wanapum Basalt, and Saddle Mountains Basalt. No units of the Imnaha or Wanapum were found in the map area. The Grande Ronde, from oldest to youngest, has been further divided into the informal R_1, N_1, R_2, and N_2 magnetostratigraphic units. The only flows of Grande Ronde Basalt identified were R_1. Saddle Mountains flows include the basalt of Feary Creek (relative age uncertain) and, from oldest to youngest, undivided flows of the Wilbur Creek Member and Asotin Member, the basalt of Weippe, and the basalt of Craigmont. Marginal to, underlying, and interbedded with the basalt sequence are the sediments of the Latah Formation.

Samples of basalt units were collected for chemical analysis; magnetic polarities of some units were determined in the field. Selected sample locations shown on the map include our samples and some samples collected by V.E. Camp from 1978 to 1980. Analytical results for these samples and for others collected on the quadrangle are published in Kauffman (2004b). Some of the samples were collected from outcrops in areas mapped as landslides (*Qls*). Although probably not in place, they give an indication of units present in the area. Several of Camp's samples were submitted to Geochron Laboratories Division, Krueger Enterprises, Inc., for whole-rock K-Ar age determinations in 1984. Results for these age determinations, cited below, were provided by V.E. Camp (written commun., 2002).

Saddle Mountains Basalt

Tcg Basalt of Craigmont (Miocene)—Fine- to medium-grained basalt. Common plagioclase phenocrysts 2-5 mm, rarely 7-10 mm; scattered to uncommon olivine about 1 mm; some manganese (?) oxide cavity filling. Normal magnetic polarity. Outcrops uncommon; poorly exposed and deeply weathered to red-brown saprolite. Thickness estimated at 15-30 meters (50-100 feet), possibly thicker locally. Uppermost basalt unit forms isolated remnants west of Jaype. First identified and named by Camp (1981). K-Ar age of a dike sampled by Camp (sample VC79-214 from sec. 1, T. 31 N., R. 5 E.) is 11.9 ± 0.7 Ma.

Tfc Basalt of Feary Creek (Miocene)—Fine- to medium-grained basalt. Common to abundant plagioclase phenocrysts 2-5 mm, rarely 10 mm in length; olivine common in the groundmass of the more grainy textured variety; olivine uncommon (or less obvious) in the finer grained variety. Normal magnetic polarity. Stratigraphic position unclear from field relations, although typically spatially associated with Asotin and Wilbur Creek unit (*Taw*) and basalt of Weippe (*Twe*). Commonly invasive into Latah Formation (*Tls*) sediments that overlie basement rocks; sediments and basalt are slumped and generally mapped as Landslide (*Qls)*. Only one unslumped area mapped east of Caldwell Creek near the western edge of the map. Not sufficiently exposed to determine thickness. First identified and included in the Frenchman Springs Member by Camp (1981), although he also was uncertain of its relative stratigraphic position but indicated it appeared to underlie the Wilbur Creek Member. K-Ar ages from two samples collected by Camp (samples VC79-349 and VC79-704) are 11.9 ± 0.7 and 11.2 ± 0.7 Ma. The samples are located in sec. 9, T. 38 N., R. 4 E., John Lewis Mountain 7.5' quadrangle, and sec. 26, T. 38 N., R. 4 E., Whiskey Butte 7.5' quadrangle, respectively. These dates indicate that the basalt of Feary Creek is

Saddle Mountains Basalt in age and similar to the age determined for the basalt of Craigmont noted above.

Tfc_d Dikes of basalt of Feary Creek (Miocene)—Fine- to medium-grained basalt dikes. Hand sample characteristics the same as for flows. Not found cutting other basalt units, only basement rocks.

Twe Basalt of Weippe (Miocene)—Medium- to coarse-grained basalt. Some plagioclase phenocrysts; abundant olivine crystals and clots are generally visible to the naked eye. Reverse magnetic polarity, although field magnetometer readings are commonly conflicting and weak. Similar chemically to the Pomona Member. Generally 30-45 meters (100-150 feet) thick, although may locally thicken to more than 60 meters (200 feet) in older structural depressions, and may include several flows or flow units. Commonly weathers to saprolite. Typically overlies Asotin and Wilbur Creek unit (*Taw*), although locally may lie directly on Grande Ronde Basalt or basement rocks where *Taw* is absent.

Camp (1981) included the basalt of Weippe in the Pomona Member because of the chemical similarity to Pomona flows, although no physical connection between the two was found. Analytical results of samples collected for the current project also reveal that the chemistry of the Weippe, for both major and trace elements, is nearly identical to the Pomona (Kauffman, 2004b). However, paleomagnetic directions determined for the basalt of Weippe from two sites near Grangemont are somewhat different from those determined for the Pomona flows by Rietman (1966) and Choiniere and Swanson (1979), indicating that the two units may not be coeval (Kauffman, 2004a, Table 2). Hooper (2000) noted this discrepancy in paleomagnetic direction but provided no data. One whole rock K-Ar age determination on sample 00JK054, collected during the summer of 2000 from the Grangemont quadrangle, resulted in a date of 12.9 ± 0.8 Ma (Kauffman, 2004a). This date is not significantly different from the 12 Ma age (no error given) reported for the Pomona Member by McKee and others (1977).

Taw Asotin Member and Wilbur Creek Member, undivided (Miocene)—Fine-grained, plagioclase- and olivine-phyric basalt. Scattered to common plagioclase phenocrysts 1-5 mm; rare to common olivine phenocrysts 1-3 mm. Upper part of flows commonly vesicular, with abundant small spherical vesicles, many with a pale bluish lining. Both members have normal magnetic polarity. Flows thickness ranges from 15-45 meters (50-150 feet).

Where more than one flow of these members is present, the stratigraphic sequence, from oldest to youngest, is: Wilbur Creek Member, basalt of Lapwai (included in the Wilbur Creek Member), and Asotin Member, although the complete sequence was not documented at any one location, and different combinations of the sequence occur at different locations. To the west in the Pasco Basin, the basalt of Lapwai and the Asotin mix to form the Huntzinger flow (Reidel and Fecht, 1987). Some mixing of these same units likely occurred in the Lewiston basin area (Garwood, 2001). Because of their close spatial relationship and because extremely detailed sampling would be required to separate them, the units have been combined on the map. However, analyzed samples are noted on the map and the individual units are identified in published geochemical tables (Kauffman, 2004b).

Grande Ronde Basalt

Tgr_1 Grande Ronde R_1 magnetostratigraphic unit (Miocene)—Dense, dark gray to black, fine- to very fine-grained aphyric to plagioclase-microphyric basalt. Reverse magnetic polarity, although field magnetometer readings commonly inconsistent and weak. Thin to thick slumped sedimentary interbeds (mapped as *Qls*) locally at top of R_1. Along Orofino Creek, this interbed erodes to form a prominent bench above Grande Ronde basalt cliffs. Interbed consists mostly of arkosic sand and silt, but contains scattered quartz and quartzite pebbles and cobbles.

INTRUSIVE ROCKS

Tb Basalt dikes, undivided (Miocene)—Black, aphanitic, tabular dikes that consist principally of plagioclase, augite, glass, and opaque oxides. Dikes are typically 1 m thick and intruded along inclined fractures or foliation; some show columnar joints. Some may be related to Columbia River Basalt Group; others (e.g., sample 01JK475, map no. 97) are clearly not as indicated by chemical composition (e.g., low FeO and high K_2O relative to the Columbia River Basalt Group; Kauffman, 2004b).

Tdu Dikes, undivided (Eocene)—Dike rocks of uncertain composition. Primarily placed on map on the basis of air photo interpretation. Unit likely dominated by rhyolite and dacite.

Tr Rhyolite dikes (Eocene)—Tan-weathering aphanitic to very fine-grained phaneritic rock that generally contains sparse bipyramidal quartz and euhedral feldspar phenocrysts.

Trp Rhyolite porphyry dikes and plugs (Eocene)—Highly porphyritic rhyolite in dikes and irregular intrusive masses. Phenocrysts are quartz and feldspar. Includes "granitic and quartz monzonitic dikes and sills" of Hietanen (1963b).

Tpd Porphyritic dacite dikes and plugs (Eocene)—Porphyritic dacite with phenocrysts of plagioclase, quartz, biotite, and hornblende in a gray aphanitic groundmass.

Ta Andesite dikes (Eocene?)—Dark gray, fine-grained dikes characterized by acicular hornblende and lath-shaped plagioclase. Some dikes have chilled margins and, more rarely, internal chilled contacts.

Tqs Quartz syenite (Eocene)—Medium- to fine-grained, porphyritic quartz syenite, syenite, and quartz monzonite. Similar to Eocene granite (*Tg)*, but quartz poor. Contains hornblende, clinopyroxene (as cores in hornblende), and biotite. Commonly occurs as resistant, iron-stained stocks and dikes. Locally contains miarolitic cavities. Includes unit mapped as the monzonite of Junction Lake by Childs (1982). Sample 90RL026 from Lunde Ridge just east of the map area (latitude 46.6105 N, longitude 114.9806 W) dated by the $^{40}Ar/^{39}Ar$ method gave a hornblende plateau age of 49.1 ± 0.4 Ma (L.W. Snee, written commun., 1992).

Tg Granite (Eocene)—Fine- to coarse-grained, equigranular to slightly porphyritic granite that contains equant to bipyramidal smoky quartz, white to pinkish feldspar, biotite, and sparse amphibole. Plagioclase grains are $An_{25\text{-}27}$. Contains miarolitic cavities, which are more common in associated aplite dikes. Pegmatites are rare. Contacts sharp and discordant. Weathers to form rounded boulder lags and spires. Includes the Bungalow pluton (Hietanen, 1968; Reynolds, 1991) in the center of the map, a small previously unmapped stock northwest of there (Cougar Rock stock), and the Horseshoe Lake stock in the southeast corner of the map.

Tggd Granite and granodiorite (Eocene)—Fine- to medium-grained hornblende-biotite and biotite granite and granodiorite. Hornblende-bearing rocks subordinate. Biotite 6-13 percent; hornblende 3 percent or less. Similar to Cretaceous to Paleocene biotite granodiorite (*TKbgd)* but plagioclase is more euhedral and more strongly zoned than in the Cretaceous plutons and the alkali feldspar has better developed perthite. Includes the Beaver Creek pluton northwest of the map's center and similar rocks south of the Kelly Forks fault in the eastern part of the area. Also includes gray, deeply weathered, porphyritic biotite granodiorite poorly exposed in a single stock along Calhoun Creek between Jaype and Headquarters with plagioclase phenocrysts 5-20 mm in length and unusually large (5-15 mm) round quartz phenocrysts enclosed in a fine-grained matrix. The Cook Mountain intrusive suite in the southeast part of the map contains several phases not mapped separately, including hornblende-biotite granodiorite north of Cook Mountain, fine-grained biotite granite in upper Martin Creek, and medium-grained hornblende-biotite and biotite granite with small pink potassium feldspar phenocrysts west of Moccasin Peak. Beaver Creek pluton locally contains clots of cordierite (Hietanen, 1963b) and a sample collected by Susan Wilson (map locality BCP) was dated by the U-Pb TIMS method at 46.4 ± 0.5 Ma (W.C. McClelland, written commun., 2002; Burmester and others, 2004).

Tggf Fine-grained biotite granite and granodiorite (Eocene)—Fine-grained biotite granite and subordinate granodiorite exposed in and near fault zones in northwestern part of area. Typically lineated and mylonitic. Biotite 5 percent or less. SHRIMP U-Pb zircon age of 48.5 ± 0.4 Ma determined from sample 00RL553 collected along Tamarack Ridge (map locality TR) north of the Benton Creek fault near western map boundary (W.C. McClelland, written commun., 2003; Burmester and others, 2004).

Tdi Diorite (Eocene)—Dark gray, medium-grained, hornblende-biotite diorite or quartz diorite in and near Beaver Creek pluton. Plagioclase is strongly zoned (An_{42-27}) and quartz is interstitial (Hietanen, 1963b). Accessory sphene, magnetite, apatite, and zircon.

Tgb Gabbro (Eocene)—Olivine gabbro and pyroxene-hornblende gabbro in and near Beaver Creek pluton. The olivine gabbro contains plagioclase (An_{60-65}), olivine, enstatite-hypersthene, hornblende, biotite, and pyrrhotite, and the pyroxene gabbro contains plagioclase (An_{47}), hypersthene, clinohypersthene, hornblende, biotite, magnetite, and apatite (Hietanen, 1963b).

Tbrgd Biotite-rich granodiorite (Eocene?)—Medium- to coarse-grained, equigranular to slightly porphyritic hornblende-biotite granodiorite of the Toboggan Ridge stock. Contains conspicuous books of euhedral biotite as thick as 4 mm and subhedral hornblende as long as 6 mm. Weathers to coarse-grained grus. Assigned possible Cretaceous age by Lewis and others (1992a, 1992b). TIMS U-Pb dating of zircon indicates a probable Eocene age (W.C. McClelland, written commun., 2002) as does preliminary LA-ICPMS zircon dating (R.M. Gaschnig, written commun., 2007).

TKap Aplite and pegmatite (Cretaceous or Paleocene)—Irregular bodies of intermixed, very coarse-grained biotite- or biotite-muscovite-bearing aplite and pegmatite. Generally lacks fabric.

TKmg Muscovite-biotite granite (Cretaceous or Paleocene)—Medium-grained, equigranular muscovite-biotite granite and granodiorite exposed only in the southeast corner of the map.

TKbgd Biotite granodiorite (Cretaceous or Paleocene)—Medium-grained, equigranular to slightly porphyritic biotite granodiorite exposed near south edge of map. Hornblende-bearing and tonalitic near some contacts with metasedimentary rocks. Weakly zoned plagioclase. Associated pegmatite and aplite dikes and sills are common. Similar rocks along the Lochsa River south of the map yielded TIMS U-Pb dates on zircon of 71 ± 9 Ma and 75 ± 5 Ma (Toth and Stacey, 1992). However, more recent SHRIMP dating (Foster and Fanning, 1997) and LA-ICPMS dating (Gaschnig and others, 2007) indicate a 62-55 Ma range for some, if not all, of the biotite granodiorite along the Lochsa.

TKpgd Porphyritic biotite granodiorite (Cretaceous or Paleocene)—Medium-grained biotite granodiorite and granite that contains subhedral phenocrysts of alkali feldspar 1-3 cm long. Otherwise similar to biotite granodiorite unit (*TKbgd)*. Present only near the southern map boundary.

Kbt Biotite tonalite (Cretaceous)—Foliated biotite tonalite, with minor amounts of foliated biotite- and hornblende-biotite quartz diorite. Biotite 5-15 percent; hornblende, where present, 3 percent or less.

Kqd Quartz diorite (Cretaceous)—Massive to foliated, medium- to coarse-grained, hornblende-biotite quartz diorite and minor tonalite. Distinguished by stubby hornblende crystals that locally define a linear fabric parallel to that in the host rocks. Locally contains inclusions of fine-grained hornblende diorite. Locally mylonitic, most notably in the Sheep Mountain and Junction Mountain areas near the Kelly Forks-Benton Creek fault system. Contains plagioclase (An_{36-38}; Hietanen, 1963b), quartz, 5-15 percent hornblende, and 5-10 percent biotite. Includes large intrusive body north of Headquarters described in detail by Hietanen (1962, 1963b) and the quartz diorite of Junction Mountain mapped by Childs (1982). Age of body near Headquarters is 94.6 ± 1.8 Ma based on TIMS U-Pb lower intercept (map locality HQ; W.C. McClelland, written commun., 2002).

Kbtg Biotite tonalite gneiss (Cretaceous)—Gray, moderately to strongly foliated biotite tonalite gneiss. Similar to Cretaceous biotite tonalite (*Kbt)* unit only more strongly foliated.

KYum Ultramafic rocks (Mesoproterozoic? or Cretaceous?)—Small dike- and sill-like bodies of medium- to coarse-grained pyroxenite or dunite that are in places altered to amphibole. Amphibole-rich variety is present north of Kelly Creek in the eastern part of the map area. Small body near west boundary of map is described as serpentinite and reported to contain serpentine, anthophyllite, olivine, magnetite, carbonate, talc, and chlorite (Hietanen, 1963a). Exposure on the north side of the Benton Creek fault north of Bertha Hill contains olivine, anthophyllite, talc, serpentine, chlorite, chromite, and chrome diopside. These bodies may be part of a massif-type anorthosite complex that has been extensively disrupted by faulting; if so, they would be similar in age to *Xan*. The small exposure on Green Point near the east margin of the Bungalow pluton is much less altered than the other ultramafic intrusions described above and may be as young as Eocene.

KXg Foliated granite (Paleoproterozoic or Cretaceous)—Small bodies of foliated and lineated, fine- to medium-grained biotite granite. Present only in the eastern part of the map along and north of Kelly Creek. Characteristically iron stained and pegmatite-rich. Biotite 3-6 percent; plagioclase is An_{22-27}. May be anatectic in origin (R.E. Kell, written commun., 1990). Measured $^{87}Sr/^{86}Sr$ is 1.0857 compared to typical values of about 0.71 for the Idaho batholith (Robert Fleck, written commun., 1992). This high $^{87}Sr/^{86}Sr$ ratio relative to the typical rocks of the Idaho batholith suggests formation from melting of Belt Supergroup or, alternatively, a Precambrian age.

KXtg Biotite tonalite gneiss (Paleoproterozoic or Cretaceous)—Gray, moderately to strongly foliated biotite tonalite gneiss and minor quartz diorite gneiss. Contains amphibolite layers and light and dark (biotite-rich) layers. Includes units mapped as quartz diorite orthogneiss by Childs (1982) and tonalite orthogneiss by R.E. Kell (written commun., 1990). Uncertain age; assumed to be Cretaceous, but a Proterozoic age possible given the spatial association with Paleoproterozoic quartz diorite gneiss (*Xqdg*).

ZYam Amphibolite (Mesoproterozoic or Neoproterozoic)—Black to dark gray, fine- to medium-grained, foliated hornblende-plagioclase rock. Interpreted to have an igneous protolith on the basis of uniform composition and texture and apparent cross-cutting relations at many places. Age assignment based on association with Mesoproterozoic or Neoproterozoic metasedimentary rocks east and west of the Beaver Creek pluton. Otherwise similar to other amphibolite units in the quadrangle.

Ygb Gabbro (Mesoproterozoic)—Sills, dikes, and small stocks of medium- to fine-grained, equigranular, pyroxene-hornblende gabbro. Includes gabbro body intruded into Prichard Formation (*Ysqp*) northwest of Crescendo Peak with U-Pb zircon age of 1467 Ma and a nearby gabbro body dated at about 1453 Ma (Doughty and Chamberlain, 2007).

Yam Amphibolite (Mesoproterozoic)—Black to dark gray, fine- to medium-grained, foliated hornblende-plagioclase rock. Age assignment based on association with Mesoproterozoic metasedimentary rocks of the Prichard Formation (*Ysqp*) and gabbro (*Ygb*) structurally above the northern anorthosite body (*Xan*). Apparently lacking in garnet, but otherwise similar to other amphibolite units in the quadrangle. Doughty and Chamberlain (2007) report 1467 and 1452 Ma U-Pb crystallization ages for the associated gabbro on Crescendo Ridge and a 1434 Ma metamorphic zircon age for an amphibolite sill along Cedar Creek.

YXam Amphibolite (Paleoproterozoic or Mesoproterozoic)—Black to dark gray, fine- to medium-grained, foliated hornblende-plagioclase rock. Typically contains garnet. Garnetiferous varieties studied in detail by Ziegler (1991) who reported 10-40 percent hornblende, 5-40 percent almandine garnet, 5-30 percent plagioclase, minor quartz, and minor ilmenite and rutile. Cummingtonite, biotite, sphene, apatite, clinopyroxene, and clinozoisite are present locally. Includes biotite-rich rock that occurs both as dikes and as thin borders on amphibolite dikes near pegmatitic intrusions. Biotite may result from replacement of hornblende. Major and trace element data reveal at least three compositionally distinct groups of amphibolite (Goldberg, 1983). Typically lineated, but interiors of some larger masses (e.g., on Indian Henry Ridge between Quartz Creek and Lost Ridge faults northeast of map center) are equigranular. Interpreted to have an igneous protolith on the basis of uniform composition and texture and apparent cross-cutting relations at many places. Age uncertain. Doughty and Chamberlain (2007) report a 1587 Ma U-Pb age for amphibolite east of Moses Butte, immediately north of the map.

YXamg Amphibolite gneiss (Paleoproterozoic or Mesoproterozoic)—Interlayered amphibolite and subordinate tonalite. Layering typically on the scale of centimeters. Present only in the northwest part of the map north of the Benton Creek fault.

Xan Anorthosite (Paleoproterozoic)—Light gray, medium- to coarse-grained metamorphosed anorthosite in two main bodies and several smaller ones in the northwest corner of the map. Typically foliated and layered, but also massive. Commonly deeply weathered to a white chalky powder; forms subdued topography. Described in detail by Hietanen (1963a; 1969), Nord (1973), Juras (1974), and Goldberg (1983). Typically contains two and locally three plagioclase populations (labradorite, bytownite, and andesine) along with subordinate muscovite, biotite, quartz, chlorite, sphene, magnetite, ilmenite, rutile, epidote, tourmaline, and apatite. Darker layers contain more biotite and in some places hornblende and garnet. Kyanite, sillimanite, and less common andalusite (which pseudomorphs kyanite) are also present, especially near the margins of the anorthosite. Resistant "knobs" of kyanite, or sillimanite after kyanite, are present in some contact zones with schist. Facet-grade garnet is produced from anorthosite-rich colluvium 1.5 km northwest of Boehls Butte in the northwest corner of sec. 30, T. 41 N. R. 5 E. The complex mineralogy in the anorthosite is due to high-grade metamorphism and hydrothermal alteration

(Carey and others, 1992; Mora and Ramseyer, 1992; Mora and others, 1999). Major elements, trace elements, and low initial $^{87}Sr/^{86}Sr$ ratios (measured average of 0.7046; Heath and Fairbairn, 1969) confirm that the anorthosite is igneous in origin (Goldberg, 1983). Foliated varieties of anorthosite appear to have oxygen isotope ratios consistent with igneous origin but megacrysts in massive varieties have oxygen isotope ratios consistent with flow of meteoric-hydrothermal fluid shortly after the last metamorphic event (M3; Walker, 1993; Mora and others, 1999).

Zircons extracted from the northern anorthosite body 1.2 km north of the northern map boundary yield a well-defined chord with an upper intercept age of 1787 ± 2 Ma (Doughty and Chamberlain, 2007). These new data refine the minimum U-Pb age of 1625 Ma of Reid and others (1973) and strengthen the case that the anorthosite is part of the pre-Belt basement of North America. An enigmatic set of small deformed dikes and sills of pegmatitic anorthosite intruded the metamorphosed rocks of the Prichard Formation (*Ysqp*) along Cedar Creek. The origin of these bodies is unclear, especially given that pegmatitic phases of the anorthosite have not been recognized elsewhere. Perhaps remobilization of the anorthosite during later metamorphism or a separate magmatic or hydrothermal event produced these dikes and sills in a manner similar to production of the megacrysts in the massive anorthosite varieties. Also problematic is that detrital zircons from several quartzite masses in and near the anorthosite are younger than the anorthosite, as described in the following sections.

Xqdg Quartz diorite gneiss (Paleoproterozoic)—Gray, moderately to strongly foliated hornblende-biotite quartz diorite gneiss. Contains amphibolite layers and light and dark (biotite- and hornblende-rich) layers. Present only in the northwestern part of the area. U-Pb zircon age of 1860 Ma obtained from a sample east of Floodwood Creek near the west end of the Smith Ridge syncline (Vervoort and others, 2007).

SYRINGA METAMORPHIC SEQUENCE

The Syringa metamorphic sequence consists of amphibolite facies metasedimentary rocks that are unlike equivalent grade metasedimentary rocks of the Belt Supergroup. The most distinctive feature is the abundance of feldspar-poor quartzite, common south of the area along the Clearwater River near the town of Syringa (Lewis and others, 1992b, 1998). The low feldspar content contrasts sharply with that in quartzite of the Belt Supergroup, most of which contains 15 percent or more feldspar. Hietanen (1962, 1963a) mapped the Syringa sequence in the quadrangle as metamorphosed Belt rocks (mostly Revett Formation quartzite). We assign these rocks to the Syringa sequence based on the abundance of feldspar-poor quartzite. This assignment is substantiated by detrital zircon age spectrum from a quartzite that differs from the detrital zircon age spectrum of nearby Revett quartzite (see *Zqs* below). Although the Syringa sequence lacks many of the lithologies typical of the lower and middle parts of Windermere-correlative strata 150 km to the south dated about 685 Ma (Lund and others, 2003), it does appear to be correlative to upper Windermere strata (Umbrella Buttes Formation) in the Gospel Hump Wilderness 100 km to the south. The Syringa sequence is nearly continuous from those rocks through the Elk City and Kooskia 30' x 60' map areas into the area directly southwest of the Headquarters map. This correlation is substantiated by a concordant age of about 680 Ma from a single detrital zircon grain in quartzite west of Dent, 35 km west of the map area, and three similar ages from the Kooskia area (P. Oswald and J.D. Vervoort, written commun., 2006). The lack of similarly young grains in such quartzite at Bertha Hill (BH sample locality on map; Lewis and others, 2007) is attributed to low abundance of such grains.

Zqs Quartzite of the Syringa metamorphic sequence (Neoproterozoic)—Quartzite and subordinate schist. Layers decimeter to meter thickness common. Quartzite characteristically pure (97-99 percent quartz) and coarse grained, although some finer grained; thin layers contain up to 15 percent feldspar. Resembles vein quartz except typically has large mica flakes well aligned between tabular quartz grains. Biotite and muscovite typically 1-5 percent. Concentrations of biotite within quartzite may mark relict bedding. Locally contains garnet or sillimanite. Detrital zircon sample from east of Bertha Hill, west of the map center (BH on map), lacks 1.5-1.6 Ga ages that Ross and Villeneuve (2003) have shown characterize western Belt Supergroup samples such as the Revett Formation (Lewis and others, 2007). Results were more similar to Laurentian zircon populations that characterize easterly derived facies of the Belt, such as the Neihart Formation (Mueller and others, 2003).

Zss Schist and gneiss of the Syringa metamorphic sequence (Neoproterozoic)—Muscovite-biotite schist and gneiss interlayered with quartzite of the Syringa sequence (*Zqs*). Locally contains sillimanite and garnet. Closely resembles Mesoproterozoic schist and gneiss (*Ysg)* and map distribution is based on the association with quartzite of the Syringa sequence.

Zcss Calc-silicate rocks of the Syringa metamorphic sequence (Neoproterozoic)—Calc-silicate gneiss and subordinate calc-silicate quartzite. Contains quartz, plagioclase, diopside, and actinolite. Closely resembles Mesoproterozoic calc-silicate rocks (*Ycs*) and assignment is based on the association with quartzite of the Syringa sequence (*Zqs*).

BELT SUPERGROUP

Belt formations can be traced with some certainty from northeast of the map southwestward to near the mouth of Black Canyon at the confluence of the North Fork Clearwater River with Kelly Creek, and westward to Pole Mountain (north-central part of map). A composite section for this northeast part of the area is described and illustrated in Burmester and others (1998). These formations can also be traced west discontinuously to the confluence of Cedar Creek and the Little North Fork of the Clearwater, despite increased metamorphic grade. Low metamorphic grade rocks without garnet or abundant calc-silicate minerals are described below. Rocks that are moderate (garnet) metamorphic grade but can be correlated with lower grade units are given metamorphic primary names and described as “Metamorphosed Belt Supergroup”, or, where formational assignments cannot be made, as “Metamorphosed Belt Supergroup?”.

Ywu_2 Wallace Formation, upper member 2 (Mesoproterozoic)—Locally calcareous quartzite, siltite, and argillite preserved only in the Chamberlain Mountain-Gospel Hill area. The uppermost part of the unit is sparsely calcareous, cross-laminated white quartzite with vertical extension fractures and interbedded subordinate siltite and argillite. Beds are a few centimeters to decimeters thick, commonly with ripple surfaces, and have abundant soft-sediment deformational structures including loaded bases and ball-and-pillow structures. Grades downward into lenticular couplets and microlaminae of dark green siltite and light green argillite and rare fining-upward planar-laminated quartzite and siltite beds 1-20 cm thick. Straight-sided desiccation cracks in argillite filled with the dark siltite are common. Correlated with the lower part of the Shepard Formation (Lemoine and Winston, 1986) 30 km northeast of the map.

Ywu_1 Wallace Formation, upper member 1 (Mesoproterozoic)—Argillite, siltite, and phyllite. Unit typically consists of parallel microlaminated and laminated black to dark gray argillite, and grayish white siltite and black argillite couplets. Some sections expose 10- to 30-cm-thick tabular siltite layers and dark gray siltite and argillite with rare cross-lamination and rippled surfaces. Small silt-filled desiccation cracks are ptygmatically folded; larger ones are straight sided. Scapolite is present in some black argillite, especially near the base of the unit. As metamorphic grade increases to the southwest, the rocks become phyllitic and contain chloritoid porphyroblasts. Stratigraphically equivalent to the Snowslip Formation to the northeast (Lemoine and Winston, 1986) but differs by having abundant dark gray argillite and lacking redbeds.

Ywm Wallace Formation, middle member (Mesoproterozoic)—Tan-weathering, grayish white, dolomitic siltite and fine-grained quartzite overlain by black argillite in pinch and swell couplets and rare couples ("black and tan" rock type), brownish orange-weathering carbonate-bearing white quartzite, and greenish gray siltite and argillite. Sedimentary structures include microlamination, ripple cross-lamination, small-scale cross-bedding, shallow channels, water-expulsion structures, and load casts. Contains minor scapolite. Beds of syndepositional breccia and layers of nonstratified breccia (shown as hollow triangles on map) occur at or near top of member. The breccia is composed of clasts of black- and tan-weathering argillite and siltite, white- and brownish orange-weathering quartzite, and rusty-weathering dolomitic siltite in a carbonate-rich, brownish orange matrix. Angular clasts are up to several meters across; rounded ones are pebble to boulder sized. Some large clasts are deformed internally, and soft-sediment folds occur in bedded rocks below breccia zones. Thickness of breccia zones ranges from 1 m to more than 200 m. Stratification of breccia zones is parallel with enclosing rocks, which suggests deposition by multiple debris flows. However, in a study northeast of the area, Collins (1999) concluded that they formed after deposition of the Wallace Formation by intrastratal faulting, possibly along Proterozoic listric normal faults within the Belt basin.

Ywl Wallace Formation, lower member (Mesoproterozoic)—Highly varied unit consisting of couples and couplets of siltite, argillite, fine-grained white quartzite, silty dolostone, dolomitic siltite, and limestone. Subordinate gray quartzite and black argillite. Locally contains scapolite. Lower part predominately wavy microlaminated to thin couplets of noncalcareous green siltite and light green argillite. Upper part dominated by siliciclastic to carbonate cycles consisting of white, fine-grained noncalcareous and calcareous quartzite, commonly 10-20 cm thick, with both planar and ripple cross-laminations and low-angle cross-beds, overlain by tan-weathering, green silty dolostone or dolomitic siltite. Thin quartzite beds throughout the unit typically exhibit vertical segmentation gaps where carbonate has been removed. Brown to orange-weathering, gray, conchoidally fracturing dolostone scattered throughout; gray laminated or massive-weathering limestone with characteristic vertical "molar-tooth" structures common. Higher in unit, oblong carbonate "pods" both parallel and perpendicular to bedding are more common within massive green siltite and silty dolostone. Tan-weathering pinch-and-swell couplets of gray quartzite and black argillite ("black and tan" rock type) typical of the middle member of the Wallace locally present, particularly high in the lower member. Good exposures in the Hoodoo Pass area near the northeast corner of the map.

Ysr St. Regis Formation (Mesoproterozoic)—Light brown, weakly phyllitic siltite, argillite, and subordinate quartzite. Typically siltite and argillite couplets, but with very thin (2-5 cm) and rarer thin (10-20 cm) tabular fine-grained quartzite beds with argillite caps. Locally contains mudcracks and mudchips, although most are obscured by metamorphism. Scattered brown weathering millimeter-scale dolomitic silt stringers in places in upper part of unit. Metamorphic grade increases to south and at Hidden Creek unit contains beds with epidote. Cleavage typically at a high angle to bedding.

Yrb Revett and Burke formations, undivided (Mesoproterozoic)—Light gray feldspathic quartzite and subordinate thin interbeds of muscovite-biotite schist and phyllite. Typically decimeter- to rare meter-thick beds. Plagioclase more abundant that potassium feldspar. Thick beds of quartzite correlated with the Revett Formation are generally tabular, and exhibit prominent cross-stratification in some outcrops along the North Fork Clearwater River downstream from the mouth of Deception Creek. Unit includes rocks previously correlated with Ravalli Group (Day, 1975; Childs, 1982; R.E. Kell, written commun., 1990).

METAMORPHOSED BELT SUPERGROUP

With increasing metamorphic grade, argillaceous rocks form phyllite and schist whereas carbonate-bearing quartzitic rocks form calc-silicate quartzite, granofels, and gneiss. Original color and fine sedimentary structures are destroyed, but in most places penetrative deformation is slight and bedding thickness, general character, and protolith composition are still recognizable. Units are named on a lithologic basis, followed by correlations with lower-grade equivalents.

$Ycwu_2$ Calc-silicate rocks, upper member 2 of the Wallace Formation (Mesoproterozoic)—Thinly bedded (centimeter-scale) calc-silicate quartzite, calc-silicate gneiss, calc-silicate granofels, biotite-muscovite schist, and biotite gneiss. Contains diopside, actinolite, and subordinate hornblende and scapolite. Thought to be metamorphic equivalent of Ywu_2 based on stratigraphic position and lateral continuity.

$Yswu_1$ Schist and phyllite, upper member 1 of the Wallace Formation (Mesoproterozoic)—Garnet-muscovite-biotite schist and phyllite, and rare diopside gneiss and calc-silicate hornfels. Scapolite present west of Five Lakes Butte and chloritoid common throughout; growth of both was across the schistosity and therefore after deformation. Garnet more abundant in this unit than in other pelitic units in quadrangle. Contains staurolite and kyanite north of Quartz Creek fault (Childs, 1982) and kyanite south of Pole Mountain in the north-central part of the map (Hietanen, 1968). A micaceous cleavage is axial planar to upright folds at intermediate grade; and schistosity is generally at some small angle to compositional layering in the highest grade rocks. Previously mapped as schist within the Wallace Formation by Hietanen (1968) in the Pole Mountain area. Considered metamorphic equivalent of Ywu_1 based on stratigraphic position and lateral continuity, with the change in unit at the garnet isograd.

Yqcw Quartzite and calc-silicate rocks of the Wallace Formation, undivided (Mesoproterozoic)—Fine-grained feldspathic quartzite, calc-silicate gneiss, biotite granofels, and minor schist. Contains actinolite south of Pole Mountain (north-central part of map). Diopside gneiss and granofels locally contain relicts of pod and ribbon structures. Metamorphic equivalent of lower and middle members of the Wallace Formation (*Ywl* and *Ywm*) based on stratigraphic position, composition of protolith, and relict sedimentary structures.

Ysqw Schist within quartzite and calc-silicate rocks of the Wallace Formation (Mesoproterozoic)—Garnet-muscovite-biotite schist. Subunit of *Yqcw* mapped only in a small area north of Dworshak Reservoir at the west edge of the quadrangle. Sillimanite and abundant garnet in unit to the west in the Potlatch quadrangle (Lewis and others, 2005). Correlation with Wallace Formation based on intimate association with rocks with carbonate protolith.

Yqw Quartzite of the Wallace Formation (Mesoproterozoic)—Fine-grained feldspathic quartzite, carbonate-bearing quartzite, calc-silicate quartzite, biotite granofels, and carbonate and calc-silicate breccia. Layering on a centimeter to decimeter scale. Contains quartz, feldspar, biotite, actinolite, diopside, and scapolite. Breccia is like that described as synsedimentary in *Ywm* unit and also shown with hollow triangles but contains calc-silicate minerals. Thickness of breccia zones ranges from 1 m to more than 200 m. Metamorphic equivalent of middle member of Wallace Formation (*Ywm*) based on composition, relict sedimentary structures, breccia, and stratigraphic position.

Ycsw Calc-silicate gneiss of the Wallace Formation (Mesoproterozoic)—Calc-silicate gneiss and granofels. Contains quartz and plagioclase and various amounts of actinolite, diopside, hornblende, calcite, and scapolite. Green stripe appearance attributed to actinolite or diopside concentrations that follow carbonate distribution in siltite and argillite couplets of protolith. Hornblende common only near intrusive rocks. Probable metamorphic equivalent of *Ywl* because it is more thinly layered and richer in calc-silicate minerals than the overlying quartzite of the Wallace Formation (*Yqw*).

Ysrv Schist of the Ravalli Group (Mesoproterozoic)—Fine- to medium-grained muscovite-biotite schist. Most likely metamorphosed St. Regis Formation (*Ysr)* based on stratigraphic position.

Yqrv Quartzite of the Ravalli Group (Mesoproterozoic)—Light gray feldspathic quartzite in layers several cm to 1 m thick and interbedded subordinate phyllite or schist. Likely dominated by metamorphic equivalents of the Revett and Burke Formations (*Yrb*, middle and lower parts of the Ravalli Group) but probably includes metamorphosed St. Regis Formation as well (*Ysr*, upper part of Ravalli Group). Previously correlated with Ravalli Group (Day, 1975; Childs, 1982; R.E. Kell, written commun., 1990). Contact with Revett and Burke (*Yrb*) is drawn at the estimated garnet isograd. Garnet rare in unit overall. The quartzite is typically fine grained and friable and forms tabular layers with internal planar and cross lamination. Plagioclase feldspar predominates over potassium feldspar. As metamorphic grade increases toward the southwest, feldspar content and grain size increase, and quartz-muscovite-biotite schist is interbedded with the quartzite. In the middle part of Black Canyon, near the mouth of Elizabeth Creek (center, eastern half of map), the unit consists of medium-grained quartzite in decimeter- to meter-thick layers with lesser amounts of biotite schist. In this area, metamorphic grade and deformation are low enough that original sedimentary structures are preserved. These include large channels, dune bedforms, and much more prominent lenticular bedding than the flat, aggradational bedding of the *Yrb* quartzite of upper Black Canyon but similar to *Yrb* exposures north of Trap Point in the northeast part of map. To the west, in the Snow Creek area (north center), the unit includes quartzite beds 1 m thick at the base of upward fining and thinning cycles. Apparent coarsening downward of the quartzite may be an artifact of increased recrystallization southward. The section west of Snow Creek, described in more detail by Burmester and others (1998), is about 2,500 m thick.

Ysqp Siltite, quartzite, fine-grained schist, and carbonate-bearing rocks of the Prichard Formation (Mesoproterozoic)—Sulfide-rich dark gray siltite, light gray to white quartzite, dark gray fine-grained schist, and gray carbonate rocks. Unit discontinuously surrounds the main body of the Boehls Butte anorthosite (*Xan*) in the northwest corner of the area, and is probably everywhere in fault contact with it and accompanying rocks of the Boehls Butte Formation. Intruded by stocks of pyroxene gabbro (*Ygb*) east of Goat Mountain at the northern edge of the map and across Cedar Creek to the south and contains concordant masses of amphibolite (*Yam*) at other locations. Siltite contains quartz, plagioclase and biotite, and various amounts of potassium feldspar, muscovite, actinolite, and graphite. Hietanen (1963a) referred to these rocks as fine-grained biotite quartzite; they are slightly coarser grained than lower-grade siltite typical of the Prichard Formation north of the area. Contrasting light and dark layers in some strata may be carbonaceous banding found widespread in the Prichard (e.g., Huebschman, 1973). Siltite is characterized, in comparison to other metasedimentary rocks in the immediate vicinity, by finer grain size (typically less than 0.5 mm) and apparent low levels of strain. Siltite grades into semi-schist, or fine-grained schist where more micaceous, or is intercalated with it. Preservation of fine grain size and weakness of the metamorphic fabric in these rocks may be due more to protolith composition than to low intensity of metamorphism. Quartzite is most abundant east of Goat Mountain but also is present on Stocking Meadows Ridge southwest of Goat Mountain. Quartzite east of Goat Mountain is white, coarse-grained, and contains 5-15 percent feldspar. The quartzite intervals are thickest along Monumental Buttes north of the map. They thin southward into the map east of Goat Mountain where they are intercalated with siltite and semi-schist. To the east toward Crescendo Peak, the quartzite contains increasing amounts of siltite, which retains relict bedding but locally has a schistosity at an angle to bedding. Quartzite body south of O'Donnell Creek (within the northern anorthosite body and labeled "*Ysqp?*" on map) contains numerous detrital zircons with $^{207}Pb/^{206}Pb$ ages the same or slightly younger than the age of anorthosite (*Xan*) (Doughty and Chamberlain, 2007). On this basis, it could be assigned to either the *YXqcb* unit or the *Ysqp* unit and be either depositional on the anorthosite (*Xan*) and Boehls Butte schist (*YXsb*) or in fault contact with them. The carbonate rocks are most abundant along Cedar Creek, south of Goat Mountain, but also are found to the east along the Little North Fork of the Clearwater River (Hietanen, 1963a) and along the northwest flank of Stocking Meadows Ridge. Included are feldspathic siltite, calc-silicate marble, marble, and quartzite that contain abundant diopside, actinolite, plagioclase, quartz, biotite, and calcite and lesser amounts of tremolite, scapolite, graphite, potassium feldspar, phlogopite, and staurolite. Spectacular exposures along the Cedar Creek road contain about 470 m of calcareous rocks in beds 2-50 cm thick that have been intensely refolded (Hietanen, 1963a). However, unlike folds in nearby schistose rocks, folds in this section have a wide variety of attitudes and lack visible penetrative fabric such as axial plane cleavage.

Hietanen (1963a) originally correlated unit *Ysqp* with the Prichard Formation, but later placed it within the pre-Belt Supergroup Boehls Butte Formation (Hietanen, 1984). Freeman and Winston (1987) speculated that the thick quartzite layers along Monumental Buttes just north of the map could correlate with the Neihart Quartzite and be the basal formation of the Belt Supergroup. However, our mapping indicates that this quartzite is part of unit *Ysqp* and most likely correlates with unit E of the Prichard Formation, well up from the base of the Prichard. The lithologic similarity of *Ysqp* and the Prichard and Aldridge formations makes a compelling case for correlating them, as does the presence of geochemically similar mafic intrusions (Goldberg, 1983) in each. The 1467 and 1452 Ma ages of two *Ygb* gabbro bodies (see *Ygb* description) indicates that the mafic intrusions are Mesoproterozoic. Although the Prichard Formation is predominately a succession of fine-grained deep-water turbidites, thick intervals of shallow water, less feldspathic quartzite occur in the middle and upper parts of the lower Prichard Formation across the basin (Cressman, 1989; Finch and Baldwin, 1984) and are exposed in the Pine Creek area about 65 km to the northwest, where they are interpreted as shelf sands (St. Godard, 1998). Furthermore, calcareous argillite and limestone were deposited along the eastern edge of the Belt basin in the Prichard Formation and in the Prichard-equivalent Greyson Formation, Altyn Formation, and Newland Formation in the Helena embayment (Cressman, 1989; Finch and Baldwin, 1984, Zieg, 1986). A similar environment may have existed along the southwestern edge of the basin such that the protoliths of the calc-silicate and marble of this unit (*Ysqp*) were deposited in a mixed siliciclastic carbonate shelf environment. Quartzite north of the map at Monumental Buttes contains a suite of detrital zircons with a $^{207}Pb/^{206}Pb$ age distribution that is similar to the distribution of detrital zircon ages from a sample of the Prichard-equivalent Aldridge Formation (Doughty and Chamberlain, 2007; cf., Ross and Villeneuve, 2003).

METAMORPHOSED BELT SUPERGROUP(?)

Highly deformed amphibolite-facies metasedimentary rocks exposed in the southern part of the map include units that are tentatively correlated with the Belt Supergroup and other units that are more difficult to correlate. In many places, especially in the central and eastern parts, the units below differ little from “Metamorphosed Belt Supergroup” units described above, but correlation with Belt units is more tenuous because of separation from them by faults or because of more internal disruption. The gneiss and schist unit (*Ygs*) is most likely metamorphic equivalent of the upper Wallace or St. Regis formations. The calc-silicate gneiss map unit (*Ycg*) is probably the equivalent of the middle and lower parts of the Wallace Formation (*Ywm* or *Ywl*) as suggested by Hietanen (1963a, 1963b), or carbonate-bearing rocks of the upper part of the Wallace (*Ywu*$_2$). Quartzitic intervals probably represent quartzite-rich portions of the middle Wallace Formation (*Ywm*) or parts of the underlying Ravalli Group (*Yrb*).

Calc-silicate rocks (*Ycs*) and schist and gneiss (*Ysg*) units in the southwestern part of the map also likely have Belt-age protoliths, but direct correlation is even less certain. Detrital zircon ages from *Ycs* rocks south of the Beaver Creek stock (map locality BC), and within *Ysg* along Snake Creek in the southwestern part of the area (map locality SC) are similar to ages from Belt Supergroup samples (Lewis and others, 2007). These rocks were mapped as Wallace Formation by Hietanen (1963b) but they differ from the Wallace in that the calc-silicate (*Ycs*) contains less quartz and is in thinner layers within *Ysg*. Because these units are mapped in close spatial association with Neoproterozoic rocks of the Syringa metamorphic sequence we suspect they are high in the Belt section and perhaps metamorphic equivalents of the Libby Formation.

Most problematic are the calc-silicate rocks (*Ycs?*) between the Benton Creek and Canyon faults, east and west of the Beaver Creek stock. East of the Beaver Creek stock, *Ycs* is thinly laminated and contains apple green diopside. West of the Beaver Creek stock it contains a distinctive graphitic marble. These textures and compositions are unlike any known in the Belt Supergroup. Likewise, the associated gneiss and schist (*Ysg*) has less quartzite than typical of the fine-grained units that are in the middle of the Belt Supergroup. A detrital zircon sample from along the North Fork east of the Beaver Creek stock (sample NF on map) contained 22 grains between 1350 and 1750 Ma (Lewis and others, 2007), permissive for a Belt Supergroup protolith. However, the sample also contained 16 grains between 1400 and 1350 Ma and 24 grains between 1350 and 800 Ma. The relatively young (<1400 Ma) zircons in this sample could reflect a young protolith that postdates the Belt-Purcell Supergroup, but these zircons are characterized by Th/U <0.1, consistent with zircon growth during metamorphism. The near concordance of most of these analyses makes it unlikely that lead loss or zircon growth during the Cretaceous is the cause of the young ages. More likely, a late Proterozoic event (or events) affected either the rock or the source of the detrital zircons. The protolith could be Belt, but the paucity of grains with high Th/U analyses makes it difficult to compare the age distribution with Belt samples. At present we tentatively assign these rocks to the Belt Supergroup, but recognize that a younger age is permissible. Additional uncertainty in unit assignments in this region results from structural complexity along the Kelly Forks-Benton Creek fault system.

Ysg Schist and gneiss (Mesoproterozoic)—Muscovite-biotite schist that grades into less abundant schistose biotite gneiss. Contains quartz, plagioclase, and biotite as well as various amounts of potassium feldspar, muscovite, and garnet. Ilmenite, rutile, graphite, and chlorite are present locally (Ruendal, 1987). Typically sillimanite-rich, in contrast to the *YXsg* and *Ygs* units. Andalusite reported from a single locality about 5 km south of Headquarters (Ruendal, 1987) might be due to intrusion of nearby *Tggd* stock. Ruendal (1987) reported muscovite and potassium feldspar intergrown in the presence of quartz and sillimanite (indicating breakdown of muscovite and conditions above the second sillimanite isograd) in three localities near Headquarters and one locality near the west edge of the map. Garnet abundant west of Democrat Mountain in the southwest part of the map but generally less common than in the $Yswu_1$ unit. Two garnet types are present: small, vitreous, lavender, and euhedral, and larger than 1 cm, opaque, rusty red, and flattened. Compositional layering is probably transposed bedding. Unit is spatially associated with *Ycs* and is perhaps the metamorphic equivalent of the Libby Formation.

Ycs Calc-silicate rocks (Mesoproterozoic)—Massive, orange weathering granofels, calc-silicate gneiss, amphibolite, and minor amounts of garnet-biotite schist and gneiss. Rocks typically contain quartz and anorthite-rich (An_{80-90}) plagioclase (Ruendal, 1987) and various amounts of diopside, actinolite, hornblende, biotite, potassium feldspar, garnet, and sphene. Parting is generally thick. Includes graphitic marble horizon north of the Benton Creek fault with graphite crystals as large as 3 mm across. Compositional layering and range in grain size distinguish hornblende-rich metasedimentary amphibolite from more homogeneous rock of the metaigneous amphibolite (*YXam and Yam*). Hietanen (1963a, 1963b) previously correlated these rocks with the Wallace Formation. Unit is spatially associated with *Ygs* and is perhaps the metamorphic equivalent of the Libby Formation.

Ygs Gneiss and schist (Mesoproterozoic)—Schistose biotite gneiss that grades into muscovite-biotite schist. Contains quartz, plagioclase, and biotite and various amounts of potassium feldspar, muscovite, and garnet. Compositional layering is probably transposed bedding. Locally migmatitic in the drainages of Hemlock Creek, Middle Creek, and Beaver Dam Creek in the south-central part of the area. Unit is spatially associated with *Ycg*. Mapped as Wallace Formation by Hietanen (1963b); a likely correlative for most of the unit is the upper member of the Wallace, although some may be metamorphosed St. Regis Formation.

Ycg Calc-silicate gneiss (Mesoproterozoic)—Centimeter-scale layered calc-silicate gneiss, layered granofels, calc-silicate quartzite, and minor amounts of garnet-biotite schist and gneiss. Parting is generally thicker than internal layering. Hietanen (1963a, 1963b) previously correlated these rocks with the Wallace Formation. Some layers have undulating boundaries that may be relict pinch and swell structures characteristic of middle member Wallace Formation (*Ywm*). Some thicker beds have brown-stained ellipsoidal holes that may be relict carbonate pods characteristic of lower member Wallace Formation (*Ywl*), and small bodies intimately associated with smaller swaths of gneiss and schist (*Ygs*) might be high-grade equivalents of upper member Wallace Formation (Ywu_2).

Yqgq Quartzitic gneiss and quartzite (Mesoproterozoic)—Generally medium- to coarse-grained, thin-layered quartzitic gneiss and feldspathic quartzite that contains various amounts of centimeter-layered biotite-feldspar quartz granofels. Grades into quartz-rich biotite gneiss where migmatized. Unit probably represents quartzite-rich portions of the middle member Wallace Formation (*Ywm*) and perhaps parts of the Ravalli Group (*Yrb*). Hietanen (1963b) mapped the *Yqg* unit as gneiss of the Wallace Formation, and Childs (1982) mapped the *Yqg* unit as quartz gneiss of the Wallace Formation.

Yqs Quartzite and schist (Mesoproterozoic)—Medium- to coarse-grained, biotite-feldspar quartzite in decimeter- to meter-thick beds. Likely dominated by metamorphic equivalents of the Revett and Burke Formations (*Yrb*, middle and lower parts of the Ravalli Group) but too highly metamorphosed and stratigraphically disrupted to be confidently correlated.

METAMORPHOSED BELT SUPERGROUP(?) OR BASEMENT(?)

YXsg Schist and gneiss (Mesoproterozoic)—Quartz-plagioclase-muscovite-biotite schist, quartz-biotite-muscovite schist, muscovite-biotite-gneiss, and gray coarsely recrystallized micaceous quartzite. Schistose rocks commonly rusty weathering due to abundant sulfides. Unit includes some bodies of amphibolite and layers of coarse-grained quartzite and rare calc-silicate quartzite that were not mapped separately. Unit is migmatitic south of Quartz Creek on Moscow Bar Ridge (center of map). Generally coarse-grained with crenulated or multiply crenulated foliation. Some coarse schist has subtle compositional layering interpreted as relict bedding; more commonly bedding appears preserved as centimeter-scale alternation of fine-grained biotite quartzite and schist. Layering mapped as bedding only where at high angles to foliation, e.g., locally in Quartz and Skull creeks. Most layers are parallel to foliation and are probably transposed bedding as indicated by rare isoclinal fold hinges to which foliation is axial planar. Locally contains sillimanite and rare kyanite and is variably garnetiferous; garnets in the northwest part of map are 1-2 cm in diameter, but elsewhere are smaller. Schist around Getaway Point and Joker Peak (north-central part, western half of map) is anomalously rich in garnets and Hietanen (1968) noted unusual abundances northwest of Larkins Peak (north central) and northwest of the mouth of Quartz Creek (central). Contains small, discontinuous sulfide-bearing quartz veins. Possible correlation with the Prichard Formation of the Belt Supergroup is based on sulfide abundance, presence of amphibolite interpreted as metamorphosed mafic sills, apparent gradational contacts with quartzite of the Ravalli Group (*Yqrv*), and on previous correlations (Childs, 1982; R.E. Kell, written commun., 1990). However, Paleoproterozoic age of quartz diorite gneiss east of Floodwood Creek (*Xqdg*) indicates that at least some of this unit pre-dates the Belt, unless the contact is depositional rather than intrusive.

YXq Quartzite (Mesoproterozoic)—Coarsely recrystallized quartzite that occurs interlayered in *YXsg*. Ranges from laminated dark and light gray to uniform white to dark gray. Includes muscovite, or biotite, or both, and rarely magnetite. Feldspar-poor. Parting typically 5-30 cm, rarely more than 1 m. Some quartzite has garnet on parting surfaces, apparently the product of thin argillaceous interlayers. Internal lamination and schist interlayers commonly tightly folded or discontinuous. Unit includes rocks previously correlated with Revett, Burke, and Prichard Formations (Hietanen, 1968; Childs, 1982), but intense deformation and lack of preservation of sedimentary features in most places make correlations uncertain. Age constraints are similar to those of the *YXsg* unit.

BOEHLS BUTTE FORMATION

Hietanen (1969, 1984) assigned quartzite and schist in the vicinity of the Boehls Butte anorthosite to the Boehls Butte Formation and suggested that they predate the Belt Supergroup. We reassigned the quartzite east of the northern anorthosite body to the Prichard Formation (*Ysqp*) and have restricted units in the Boehls Butte Formation to include only the Al-Mg schist that borders the masses of anorthosite (*Xan*), the lowermost schist that is present in the core of the Boehls Butte uplift along Floodwood Creek, and minor quartzite and calc-silicate rocks. The age of the largest mass of schist (*YXsb* along Floodwood Creek) is not well established in that the original contacts with the dated *Xan* unit could be intrusive, depositional, or tectonic. We have included small quartzite bodies that have detrital zircon ages less that that of *Xan* (Doughty and Chamberlain, 2007) in this unit because contact relations could not be established. Thus some or all of the schist, excluding the Al-Mg variety, could be Mesoproterozoic, possibly Prichard Formation. Additional studies are clearly needed to determine the true age and extent of the Boehls Butte Formation.

YXsb Schist of the Boehls Butte Formation (Paleoproterozoic or Mesoproterozoic)—Medium-grained, sillimanite-rich, muscovite-biotite schist and coarse-grained Al- and Mg-rich schist. Present only in the structurally lowest levels in the vicinity of Floodwood Creek and in contact zones with anorthosite (*Xan*). Most weathers to small (1-4 cm) platy chips and is finer grained and richer in sillimanite than the *YXsg* unit. Locally contains kyanite and staurolite (Hietanen, 1963a; Nord, 1973). Adjacent to the anorthosite, this schist is coarser grained and locally gneissic. There, it contains porphyroblasts of andesine and high concentrations of coarse-grained aluminosilicate minerals. All three phases (kyanite, sillimanite, and andalusite) are common, and the rock is enriched in Al and Mg (Hietanen; 1963a; Carey and others, 1992). Areas with abundant aluminosilicate minerals are designated with a diagonal line pattern on the map. Aluminosilicate-rich schist is most likely a contact metamorphic rock that was intruded by the Early Proterozoic anorthosite (Carey and others, 1992).

YXqcb Quartzite and calc-silicate rocks of the Boehls Butte Formation (Paleoproterozoic or Mesoproterozoic)—Poorly exposed feldspathic quartzite and calc-silicate gneiss interlayered with the *YXsb* unit.

GEOCHEMISTRY

Twenty-one samples of Miocene volcanic rocks and 67 samples of Eocene and older basement rocks were analyzed by whole-rock X-ray fluorescence (XRF) methods for this study and previous mapping efforts in the area by the Idaho Geological Survey. The locations for most of these samples are shown on the map; a complete list of volcanic rock samples and chemical results is available in a digital format (Kauffman, 2004b) as are the data for the basement rocks (Lewis and Frost, 2005; Table 1). The digital data set of Kauffman (2004b) includes analyses of volcanic rocks collected between 1978 and 1980 by V.C. Camp in a regional study of the Columbia River Basalt Group (Swanson and others, 1979a). Locations for some of Camp's samples are also shown on the map. All of the basalt samples and some of

Table 1. Major element oxide, Rb, and Sr compositions of selected units in the Headquarters quadrangle and nearby areas. FeO* is total Fe as FeO.

Samples of *TKbgd* are from Bitterroot lobe of the Idaho batholith southeast of the Headquarters quadrangle.

Unit	SiO2	Al2O3	TiO2	FeO*	MnO	CaO	MgO	K2O	Na2O	P2O5	CaO+ Na2O	Rb	Sr	source of data
					weight percent							parts per million		
Belt or pre-Belt pelitic rocks														
YXsg (n=9)	67.90	17.60	0.77	5.43	0.05	0.46	1.46	4.21	1.28	0.04	1.73	187	144	Lewis and Frost, 2005
YXsg (sample FH-16)	63.25	18.25	0.77	8.11	0.05	0.96	1.73	3.49	0.86	0.04	1.82	188	50	Goldberg (1983)
Yswu1 (n=2)	68.52	16.78	0.73	4.32	0.03	0.25	2.11	5.23	0.82	0.10	1.06	209	33	Lewis and Frost, 2005
Boehls Butte Formation pelitic rocks														
YXsb (sample 1690)	60.77	21.83	0.78	7.19	0.10	1.88	1.25	2.99	1.06	0.06	2.94			Hietanen (1963a)
YXsb (sample BBM-6)	63.15	19.29	0.81	6.74	0.04	0.70	2.96	3.19	0.30	0.04	1.00	162	22	Goldberg (1983)
Al-rich schist near Xan contact														
YXsb (sample 630)	51.65	26.42	0.12	2.03	0.10	3.35	4.79	5.10	4.41	0.01	7.76			Hietanen (1963a)
YXsb (sample 954)	56.00	27.16	0.24	2.78	0.03	4.88	1.75	1.76	4.34	0.00	9.22			Hietanen (1963a)
YXsb (sample 967)	46.04	29.20	0.24	5.01	0.20	0.68	9.00	3.60	2.99	0.00	3.67			Hietanen (1963a)
YXsb (sample 971)	56.47	25.44	0.07	1.74	0.04	4.12	2.64	1.47	6.73	0.02	10.85			Hietanen (1963a)
YXsb (sample BBG-5)	52.90	29.10	0.08	3.02	0.10	4.54	3.14	1.58	5.12	0.00	9.66	32	352	Goldberg (1983)
Anorthosite														
Xan (01MDM101; map no. 57)	50.25	30.55	0.08	0.93	0.02	14.94	0.40	0.22	3.01	0.02	17.95	4	637	Lewis and Frost, 2005
Xan (01RB169; map no. 58)	50.51	31.21	0.07	0.63	0.01	13.82	0.66	0.37	3.29	0.02	17.11	8	415	Lewis and Frost, 2005
Eocene plutonic rocks														
Tggd (90TF010; map no. 9)	71.00	15.30	0.19	1.30	0.03	1.86	0.46	4.25	4.11	0.14	5.97	114	235	Lewis and Frost, 2005
Tggd (90TF020, map no. 11)	66.90	15.70	0.51	3.36	0.04	2.39	0.89	4.42	3.80	0.20	6.19	94	330	Lewis and Frost, 2005
Tggd of Beaver Cr. pluton (n=5)	72.54	14.81	0.22	1.59	0.03	1.70	0.48	4.27	3.65	0.10	5.36	136	183	Lewis and Frost, 2005
Cretaceous-Paleocene plutonic rocks														
TKbgd of the Idaho batholith (n=19)	71.14	15.62	0.22	1.41	0.02	2.35	0.48	2.84	4.71	0.10	7.06	70	764	Lewis and Frost, 2005

the basement rocks were analyzed at Washington State University's GeoAnalytical Laboratory. The remaining samples were analyzed at U.S. Geological Survey laboratories in Denver, Colorado.

Two metamorphosed pelitic units were sampled for chemical analysis (*YXsg* and *Yswu$_1$*; Table 1). Average values of the *YXsg* unit are similar to *Yswu$_1$*, although concentrations of FeO* and CaO + Na_2O are slightly higher and MgO is lower in *YXsg*. We did not analyze any sample from *YXsb*, the lowermost schist unit, but results from sample 1690 reported by Hietanen (1963a) and BBM-6 from Goldberg (1983) are given in Table 1. These samples are similar in composition to Belt(?) pelites, but are slightly enriched in Al_20_3. Samples 1690 and BBM-6 differ significantly from the aluminosilicate-rich schist found near the anorthosite contact. Samples of the aluminosilicate schist (630, 954, 967, and 971), reported by Hietanen (1963a) and BBG-5 reported by Goldberg (1983) have dramatically higher Al_20_3 and CaO+Na_2O concentrations, and are notably enriched in MgO relative to Belt pelites (Table 1). Although these samples lack the extreme Al_20_3 and CaO+Na_2O concentrations of the anorthosite (compare with 01MDM101 and 01RB169), their compositions are clearly different from the *YXsb* schist located away from the anorthosite contact. Carey and others (1992) concluded that partial melting of pre-Belt pelitic country rock left a Mg- and Al-enriched restite surrounding the anorthosite intrusion, an explanation that is consistent with field relations.

Areas of granodiorite east of the Bungalow pluton and southeast of Gorman Hill in the southeastern parts of the quadrangle were previously mapped as Cretaceous tonalite and biotite granodiorite (Lewis and others, 1992a). Although age determinations are lacking, we have herein assigned these rocks to the Eocene *Tggd* unit on the basis of textural and chemical similarities to dated *Tggd* plutons elsewhere in the quadrangle (e.g., the Beaver Creek pluton). Analyses for two samples of the newly assigned *Tggd* unit (90TF010, map no. 9; 90TF020, map no. 11) are compared with the average values of five samples from the Beaver Creek pluton and 19 samples of the Bitterroot lobe of the Cretaceous-Paleocene Idaho batholith (Table 1). The two *Tggd* samples have major element and Rb and Sr concentrations similar to those of the Beaver Creek pluton. In contrast to the Bitterroot lobe average, both samples have higher K_2O and lower Na_2O concentrations. The most notable difference is the lower Sr concentrations of the two Tggd samples (235 and 330 ppm) relative to the average value for the Bitterroot lobe (764 ppm).

METAMORPHISM

Metamorphic grade, penetrative deformation, and recrystallization increase progressively from northeast to southwest. The garnet isograd, approximately located on the map, provides a general reference that separates weakly metamorphosed rocks from those metamorphosed at higher grade. Given that garnets in the region have a range of ages (1470 Ma, 1380 Ma, 1100-1000 Ma, and 90 Ma; Sha and others, 2004; Vervoort and others, 2007), the isograd is almost certainly composite. Garnet is most abundant in the *Yswu$_1$* unit, common in *Ysg*, but only locally abundant in *YXsg*. Kyanite is present near the north edge of the map in schist below the Boehls Butte anorthosite (*YXsb*), in the contact zone of the anorthosite, in the *YXsg* unit northwest of Larkins Peak and west of The Nub, and in the *Yswu$_1$* unit south of Pole Mountain and north of Quartz Creek (Hietanen, 1963a, 1968; Nord, 1973; Childs, 1982). Andalusite has partly replaced strained kyanite in the Boehls Butte area (Carey and others, 1992). Andalusite is also reported from a locality about 5 km south of Headquarters (Ruendal, 1987) and from northwest of Junction Mountain south of the Kelly Forks fault (Childs, 1982). Cordierite is present in the Boehls Butte area (Hietanen, 1963a; Carey and others, 1992), northwest of Junction Mountain (Childs, 1982), and as inclusions in the Beaver Creek pluton (Hietanen, 1963b). Sillimanite is abundant in the schist below the Boehls Butte anorthosite (*YXsb*), in the *Ysg* unit across much of the southern and western parts of the quadrangle (Hietanen, 1963a, 1963b), and is present in minor amounts in the *YXsg* unit in the northwestern part of the area. When metamorphism produced these minerals is not entirely clear. The earliest metamorphic event must date from ~1860 Ma intrusion of *Xqdg*, but this would be confined to its country rock, whose extent is not clear. Next and also local would be contact metamorphism of *YXsb* by the 1787 Ma intrusion of *Xan*. Also local to the Boehls Butte area may have been a Proterozoic event responsible for 1.1 Ga growth of garnet cores (Sha, 2004; Sha and others, 2004; Vervoort and others, 2005). However, it is possible that this event was more widespread and responsible for the larger, opaque garnets in *Ysg*. A 1.1 Ga metamorphic event could also explain the spread of detrital zircon ages (most are 1100-1700 Ma; Lewis and others, 2007) in the North Fork sample (NF on map) as well as the low Th/U ratios of the younger grains (see "Metamorphosed Belt Supergroup(?)" section above). Since data indicating a 1.1 Ga metamorphic even are new and may not bear on metamorphism across the entire map area, renumbering metamorphic events seems premature. However, observations attributed to M1 (below) may include products of one or all of these events.

Three metamorphic periods have been widely recognized (M1, M2, and M3; Lang and Rice, 1985a, 1985b; Carey and others, 1992). The first metamorphic event produced micaceous foliation in the higher grade rocks and is referred to as M1. Mineral textures associated with M1 are best preserved north of the area near Snow Peak where growth of garnet, staurolite, chloritoid, and kyanite is documented (Lang and Rice, 1985b); it is poorly preserved in this map. At Goat Mountain, garnet cores include rare M1 inclusion assemblages and indicate conditions of about 500°C and 5.0-6.0 kb (Carey and others, 1992; Grover and others, 1992). Grover and others (1992), Larson and Sharp (1998), and House and others (1997) have speculated that M1 metamorphism was coincident with arc magmatism and crustal shortening at about 100-80 Ma. Laser-ablation ICPMS dating of metamorphic overgrowths from the *Ycs* unit east of the Beaver Creek pluton produced a population with 85-90 Ma ages (sample locality NF; Lewis and others, 2007) which is consistent with Late Cretaceous orogeny. Whether this represents M1 or a later metamorphic event is unknown.

M2 produced peak metamorphic zones that increase in intensity from northeast to southwest. Garnet, kyanite, and sillimanite grew during this event (Lang and Rice, 1985b; Carey and others, 1992). Lang and Rice (1985a) reported pressures and temperature for M2 of 500°C and 4.5-5 kb north of the map at Snow Peak, whereas rocks from the Boehls Butte area yielded peak M2 temperatures of 650-825 C and pressures of 8-11 kb (Carey and others, 1992; Grover and others, 1992). If the 85-90 Ma metamorphic overgrowths (Lewis and others, 2007) date this event, M1 must be older than 90 Ma (perhaps Proterozoic). Alternatively, M2 could be younger than the 85-95 Ma event, and coincident with intrusion of the younger phases of the Idaho batholith (cf., Foster and others, 2001).

M3 is attributed to nonequlibrium rapid unroofing about 56-48 Ma (Carey and others, 1992; Grover and others, 1992; House and others, 1997; Foster and others, 2001). Occurrence of all three aluminum silicate polymorphs in the Goat Mountain area is attributable to isothermal decompression from high temperature and does not represent an equilibrium assemblage at T and P of the triple point. Conditions in the Goat Mountain area during M3 were around 650-750°C and 3-6 kb (Ziegler, 1991; Grover and others, 1992). Slow initial cooling after M2 followed by rapid unroofing of *Xan* and *YXsb* is reflected in oxygen isotope fractionation among minerals near Goat Mountain (Larson and Sharp, 1998). Short-lived meteoric water circulation after M3 may have facilitated rapid cooling through advection and local oxygen isotope exchange within the Boehls Butte anorthosite at ~550°C and 2-4 kb (Mora and others, 1999). As discussed in the following section, syn-M3 unroofing of pre-Belt basement rocks in the northwest part of the area was facilitated by detachment on the newly mapped Jug Rock mylonite zone, located along the eastern side of the northern anorthosite body (Doughty and Buddington, 2002; Sha, 2004; Foster and others, in press).

STRUCTURES

Several significant structures cross the quadrangle, the largest of which are shown on a regional geologic map of the area (Figure 3). The Kelly Forks fault and the Benton Creek fault are part of a major strike-slip system that crosses the central part of the quadrangle. The term Kelly Forks-Benton Creek fault system is herein used to designate one continuous structure that crosses the quadrangle north of the Bungalow pluton and south of the Beaver Creek pluton. The Packsaddle syncline trends southeast into the northern part of the map and is flanked on the south by the White Rock and St. Joe faults. In addition, there are myriads of named and unnamed faults including relatively young structures. Some of these faults exhibit

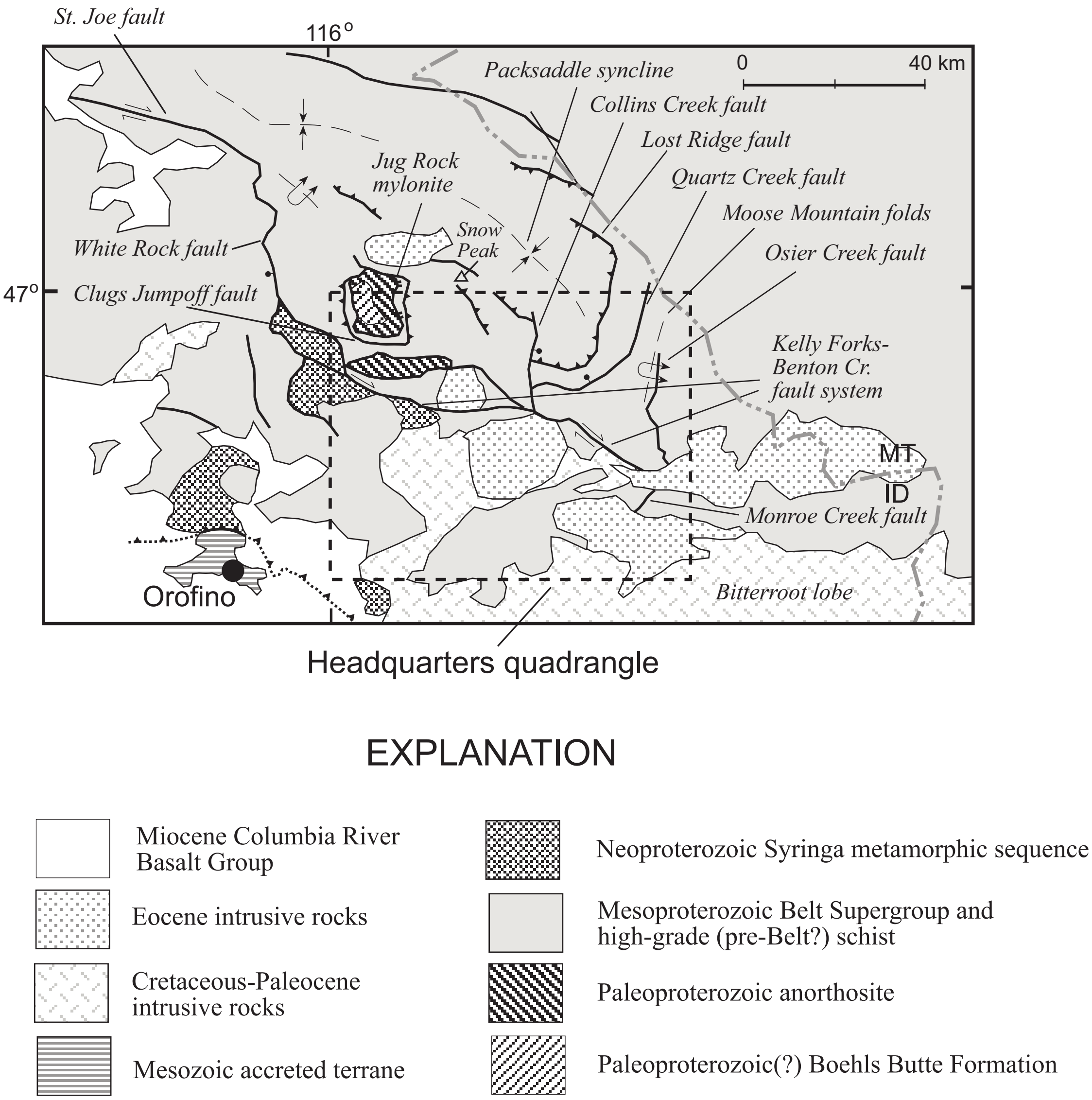

Figure 3. Simplified geologic map of the Headquarters quadrangle and surrounding area.

evidence of movement at shallow crustal levels, such as gouge, breccia, and void-filling quartz crystals. Some of these and other faults retain mylonite and ultramylonite fabrics indicative of earlier movement under higher temperature and pressure conditions. Multiple periods of motion have been suggested for some of the larger faults. An example is the Kelly Forks fault, in which major left-lateral motion is thought to have predated a subordinate amount of right-lateral motion (Childs, 1982; Kell and Childs, 1999). Other faults are inferred from contrasting rock type or incomplete stratigraphic succession. An example of an inferred fault is 7 km northeast of Pierce where metamorphosed Belt Supergroup units on the northeast (*Ycg* and *Yqg*) are juxtaposed against presumably young Belt units (*Ysg* and *Ycs*) on the southwest. To the northwest and southeast this inferred fault is obliterated by *Kqd*. It may have once merged to the north with the Kelly Forks-Benton Creek fault system prior to intrusion of the *Kqd*. The history of most of the older faults is unclear. Paleomagnetic directions derived from Missoula Group rocks in the Packsaddle syncline support at least 50° of counterclockwise rotation (Burmester and Lewis, 2003). Thus, the original orientation of stress and strain cannot be deduced from the present orientation of the earliest structures in these rotated blocks.

JUG ROCK MYLONITE ZONE AND RELATED FAULTS

One of the more impressive structures in the area is the Jug Rock mylonite zone. It is a north-south striking structure that coincides with the contact between the Al-Mg schist of the *YXsb* unit along the eastern border of the northern body of Boehls Butte anorthosite (*Xan*) and metamorphosed Prichard Formation (*Ysqp*) to the east. It separates the anorthosite and its country rocks, metamorphosed at 8-11 kb (30-40 km) and 650-750°C during M2 (Carey and others, 1992; Grover and others, 1992), from possibly lower grade (porphyroblast-free) phyllite and quartzite of the *Ysqp* unit. Top-to-the-east sense of motion, determined from S-C mylonite fabrics, extensional crenulations, and rotated porphyroclasts is consistent with this zone being part of an extensional detachment that tectonically exhumed the anorthosite during Eocene extension (Doughty and Buddington, 2002; Sha, 2004). In the hanging wall, a gradual eastward increase in metamorphic grade over a few kilometers, deformation, and amount of orthogneiss suggest that the upper plate was rotated down to the west with Eocene listric motion on the Jug Rock fault. The Jug Rock mylonite zone lacks brittle fabrics, indicating that it ceased moving before being uplifted to shallow levels (Sha, 2004). A similar sharp contrast in metamorphic grade between the anorthosite and flanking rocks exists on the northern and southern boundaries of the anorthosite, but there is no well-exposed continuous mylonite zone comparable to the Jug Rock mylonite zone present along these contacts, although mylonites have been preserved locally. Those contacts are characterized by blastomylonitic rocks with steep foliations and subhorizontal lineations. The lack of continuous preservation of mylonites is indicative of some recrystallization after shear. Kinematic indicators (extensional crenulations) suggest dextral subhorizontal shear along the northern margin (north of the area) and sinstral shear along the southern margin, which is kinematically compatible with the top-to-the-east movement along the eastern segment of the Jug Rock mylonite zone. Consequently, we conclude that the Jug Rock mylonite zone wraps around the anorthosite's northern and southern boundaries, where it turns into east-west-trending strike-slip shear zones. The western contact between the anorthosite and *Ysqp* is well located but not exposed. East of the contact, granites are mylonitized and the anorthosite contains thin mylonite shear zones. These mylonites dip gently to the east and west and yield both tops-to-the-east and tops-to-the-west kinematic indicators. West-verging mylonites also are found in the hanging wall north of the map near Widow Mountain. We infer that the west-dipping, tops-to-the-east mylonites are part of the Jug Rock mylonite zone that has been arched over the top of the anorthosite. Origin of the tops-to-the-west structures is unknown, but may relate to the White Rock fault northwest of the area. The Jug Rock mylonite zone may also be down-dropped to the west along a steep normal fault, as mapped by Hietanen (1963a).

In a similar manner, the southern body of the Boehls Butte anorthosite is juxtaposed against surrounding metamorphic rocks along ductile shear zones that, although less well exposed, appear to be like the Jug Rock mylonite zone. Bounding ductile shear zones are well exposed at the eastern extent of the anorthosite, north of the North Fork Clearwater River, where the anorthosite contact is mylonitized in a gently east-dipping shear zone with down-dip lineations. This is consistent with an extensional detachment that exhumed the southern mass of anorthosite. The southern boundary of the southern anorthosite body probably merges with the Canyon fault, but exposure is poor along that stretch of Dworshak Reservoir and the mapped fault is speculative.

CLUGS JUMPOFF FAULT

A major east-striking fault zone has been traced from between the two anorthosite bodies (*Xan*) along the southern boundary of *Ysqp* from Floodwood Creek east to Clugs Jumpoff. This fault zone separates metamorphosed but relatively undeformed Prichard Formation (*Ysqp*) to the north from schist (*YXsg*) and orthogneisses (*KXtg and Xqdg*) to the south. Slivers of anorthosite, coarse-grained aluminous schist, and mylonitic amphibolite are present along this zone of poorly exposed faults. Mylonitic rocks along the fault zone dip moderately to steeply to the south and contain subhorizontal mineral lineations. One sample from a fault on the north side of the zone exhibits kinematic indicators that suggest dextral shear. However, the attitude of the fault suggests that it may have been folded. The eastern and western extents of this fault zone are unknown. It may continue as a steep fault both to the east and west, connecting with the Canyon fault and Kelly Forks fault to the east. More likely, it may swing north along the contact between the less deformed Prichard (*Ysqp*) and the overlying schist (*YXsg*) and orthogneiss units. If so, it would have a relatively shallow dip on these northern portions and be a regional thrust fault, as depicted on this map. This hypothesized thrust places older rocks (Paleoproterozoic quartz diorite gneiss, *Xqdg*) over younger and perhaps lower grade rocks (siltite and associated rocks of the Prichard Formation; *Ysqp*).

KELLY FORKS, BENTON CREEK, CANYON, AND RELATED FAULTS

South of the southern anorthosite body (*Xan*) and unambiguous Belt strata, and north of the Syringa metamorphic sequence is a set of west-northwest- and northwest-striking faults. These include the Canyon fault and the herein named Benton Creek fault. To the east near the center of the map, these faults merge into the Kelly Forks fault. The northwest extension of the Canyon fault mapped by Hietanen (1984) was not substantiated by this study. Instead, the poorly exposed fault trends westward from Isabella Creek, rather than northwestward. The Benton Creek fault is characterized by chloritic breccia as well as mylonitic rocks. The Kelly Forks fault may continue east as far as the north end of the Bitterroot core complex (Fig. 3), but its eastward extent beyond Cayuse Creek is uncertain and it may either be obscured by younger intrusions, or motion was transferred south along some of the northeast-striking normal faults in the area, such as the Monroe Creek fault. Mylonite is more common in the west and chlorite breccia in the east along the Kelly Forks-Benton Creek fault system, indicating that uplift was greater to the west. Mylonite also is more common on northern splays of the Benton Creek fault system than on southern ones, possibly indicating that slip propagated southward during uplift. Sheath folds are well developed in the metasedimentary rocks along the eastern part of the Benton Creek fault north of the Bungalow pluton (east of Sheep Mountain in the Eagle Creek drainage).

Sheared plutons along the faults contain subhorizontal stretching lineations and have S-C fabrics indicating right-lateral motion. Ages of *Tggf* and the Beaver Creek pluton (*Tggd*) indicate that faulting was ongoing 48.5-46.4 Ma (Lewis and others, 2002b; Burmester and others, 2004). The Kelly Forks-Benton Creek fault system seems to continue westward as a zone of mylonites along Stony Creek, possibly connecting to the White Rock fault on the St. Maries and Potlatch 30' x 60' maps (Lewis and others, 2000; Lewis and others, 2005). These faults likely are part of a system that transferred Eocene extension between the northern end of the Bitterroot core complex and the southern end of the Priest River core complex (see Seyfert 1984; Doughty and Sheriff, 1992; Lewis and others, 2002a; Foster and others, 2004). It also seems likely that this fault system had a previous history. As noted above, Childs (1982) and Kell and Childs (1999) have postulated that early left-lateral motion was followed by minor right-lateral motion along the Kelly Forks fault. A quartz-biotite mylonite in the east formed early under conditions of biotite stability, with drag of folds indicating left-lateral displacement (Childs, 1982). Early left-lateral slip may have offset Syringa sequence rocks relatively eastward on the south side of the fault.

COLLINS CREEK FAULT

The Collins Creek fault is one of several high-angle faults in the central part of the area that strike north-south. The higher metamorphic grade (grain size) west of the fault suggests that the fault is a top-to-the-east normal fault. To the south, this fault apparently merges with the Kelly Forks fault. It may have moved in conjunction with right-lateral slip on the Kelly Forks fault. Little is known about this potentially significant fault and more study is warranted.

PACKSADDLE SYNCLINE

The axis of the Packsaddle syncline trends northwest from the northeast corner of the map through the Wallace and St. Maries maps (Lewis and others, 1999; Lewis and others, 2000). In the Headquarters 30' x 60' quadrangle it is deflected by north-south folds in the Pole Mountain and Bacon Peak areas in the northeast part of the map. To the northwest, the Packsaddle syncline is considerably simpler. Metamorphic grade is asymmetric across it, with a steep metamorphic gradient exposed on the south flank (Lang and Rice, 1985a, 1985b) suggesting that some deformation in the area predated early metamorphism (M1) and that the syncline achieved its present form by tilting the southwest flank northward after M2. Folding of foliations in the Boehls Butte anorthosite and surrounding schists into fold trains roughly parallel to the Packsaddle syncline may postdate M2 and likely was synchronous with formation of the syncline. Minor thrust faults south of Snow Peak (Fig. 3) strike parallel to the syncline and may also have formed at the same time. S-C fabrics in mylonitized quartzite indicate top-to-the-south-southwest transport (in present geographic framework) on these minor faults.

OPEN FOLDS AROUND POLE MOUNTAIN AND BACON PEAK

Several north-south folds are mapped between Pole Mountain and Bacon Peak (northeast part of map near northern boundary). Development of these folds may have accommodated east-west shortening synchronous with the east-directed thrusts at Five Lakes Butte, discussed below. The lateral metamorphic gradient from kyanite-bearing schist of the $Yswu_1$ unit near Pole Mountain to porphyroblast-free phyllite of the stratigraphically equivalent Ywu_1 unit east of Bacon Peak suggests that there may have been a thrust wedge that thinned eastward over this area before M2. Whether emplacement of this wedge was during folding and how it relates to the asymmetry of metamorphism across the Packsaddle syncline is unclear.

LOST RIDGE FAULT SYSTEM

The Lost Ridge fault system consists of east-west and north-south segments. The east-west segment is poorly documented. The north-south segment has multiple splays that have been mapped through the Five Lakes Butte area (Stryhas, 1985a, 1985b). Whether the north-south and east-west segments are a single system that has been folded, or two systems that appear to merge is uncertain. If it is a single system it must predate folding. Alternatively, the two segments may date from different events. The east-west segment, along with southwest-verging thrusts west of Pole Mountain to the northwest, may relate to formation of the Packsaddle syncline, described above. The north-south segment may relate to open folds between Pole Mountain and Five Lakes Butte.

QUARTZ CREEK AND WOLF CREEK FAULTS

The Quartz Creek and Wolf Creek faults strike east-northeast and omit section; net movement is thought to be normal, down-to-the-north. However, Childs (1982) suggested that the Quartz Creek structure originated as a north-dipping, dextral reverse fault that was active during folding. Thus, prior to extension and normal motion, it may have been similar to the Lost Ridge fault system.

MOOSE MOUNTAIN FOLDS

A map-scale overturned syncline cored by *Yqcw*, and an overturned anticline cored by *Yrb* and *Yqrv*, are well exposed in the Moose Mountain area (central part of eastern half of map). These are anomalous in that they are fairly tight, and overturned to the west-northwest. They may have originated during the same eastward shortening event that produced the east-verging thrust faults, but are possibly associated with unrecognized back thrusting. Alternatively, they may have formed in response to eastward driving of the Packsaddle syncline.

OSIER CREEK FAULT

The Osier Creek fault extends north-south near the eastern map boundary. This is probably a down-to-the-east normal fault as it is steep and omits *Ysr*. However, it may have had an earlier thrust history during shortening and formation of the Moose Mountains folds, possibly as a west-directed back thrust.

GEOLOGIC HISTORY

Rocks that the ~1860 Ma quartz diorite (*Xqdg*) or the ~1787 Ma anorthosite (*Xan*) intruded are the oldest in the region. The extent of the former and its relationship to the latter is unknown. The pre-anorthosite country rocks, most likely the protolith of the aluminosilicate-rich schist (*YXsb*) marginal to the anorthosite, was deposited prior to, and contact metamorphosed by, intrusion of the anorthosite. The relatively fine-grained, sillimanite-rich schist in Floodwood Creek (also *YXsb*) west of the northern anorthosite body could be either deposited on the anorthosite complex or faulted against it. Additional detrital zircon sampling in the Floodwood Creek area would help establish the age of these metasedimentary rocks. Some of the amphibolite sills in the anorthosite complex are about 1587 Ma (Doughty and Chamberlain, 2007) indicating a second pulse of magmatic activity prior to deposition of the Belt Supergroup.

Most of the fine-grained siliciclastic and carbonate-bearing clastic rocks of the Belt Supergroup were deposited between about 1470 and 1400 Ma during the Mesoproterozoic (Anderson and Davis, 1995; Evans and others, 2000). Some of the mafic sills and gabbro bodies in the metamorphic equivalents of the Prichard Formation in the northwest part of the quadrangle appear to be syndepositional and the same age as mafic sills in the Plains, Montana, area 50 km to the northeast (~1468 Ma; Doughty and Chamberlain, 2007; Sears and others, 1998). During Prichard deposition, the northwest elongate Belt-Purcell basin was flanked by a carbonate shelf along its eastern and southeastern margins. Sediment entered the basin primarily from the south and southwest and stratigraphic studies indicate that the basin shallowed toward the south (Cressman, 1989). The nature of the southwestern margin of the basin is poorly known, primarily because of Cretaceous metamorphism and probable Proterozoic metamorphism. The quartzite and carbonate-rich meta-Prichard unit (*Ysqp*) in the northwest part of the area may have been deposited either as a basin-margin facies or during a period of shallower water deposition. However, sulfides are still abundant locally, indicating recurrent periods of deposition under anoxic conditions. There is no known Prichard south of the Kelly Forks-Benton Creek fault system, suggesting that it may have at least partly controlled the extent of the early Belt basin. Higher Belt units present in the quadrangle were deposited in relatively shallow water, near or above wave base, and apparently extend more widely than the Prichard.

Deformation and metamorphism may have occurred in the quadrangle at or near the end of deposition of the Belt Supergroup as part of the East Kootenai orogeny recognized to the north in Canada (White, 1959; Leach, 1962; McMechan and Price, 1982; Höy, 1993; McFarlane and Pattison, 2000) and indicated by 1380 Ma plutonism west and southeast of the quadrangle (Evans and Fisher, 1986; Doughty and Chamberlain, 1996; Lewis and others, 2005; Lewis and others, 2007). The sixteen 1400 to 1350 Ma zircon grains with low Th/U ratios (suggestive of metamorphic origin) reported by Lewis and others (2007) from the North Fork (NF) sample may also record the East Kootenai orogeny. A second period of Proterozoic metamorphism is indicated by 1.1 Ga garnet growth recorded by Lu-Hf dating of metamorphic garnet cores in amphibolite near Goat Mountain (Sha, 2004; Sha and others, 2004; Vervoort and others, 2005). More speculatively, the five 1100 to 1200 Ma concordant and nearly concordant detrital zircon $^{207}Pb/^{206}Pb$ ages (North Fork sample; Lewis and others, 2007) from zircons with low Th/U ratios may also date from this younger metamorphic event.

Deformation and magmatism in the Neoproterozoic led to accumulation of sedimentary and volcanic rocks of the Windermere Group in northeastern Washington (Miller, 1994) and in the Gospel Peaks area 100 km south of the Headquarters quadrangle (Lund and others, 2003). Current thinking is that the Syringa metamorphic sequence is correlative with the younger part of the Windermere Supergroup (see description of Syringa above). If true, the paucity of detrital zircon grains with Windermere ages suggests absence of local volcanism, so the local tectonism may have been dominantly transform faulting between rift systems to the northwest and southeast. The older detrital zircon ages are consistent with a Laurentia source and similar to that of the Neihart and Aldridge formations (Ross and Villeneuve, 2003), suggesting rejuvenation of a regional sedimentary system that existed before Belt deposition. Neoproterozoic rifting (Colpron and others, 2002) and formation of a passive plate margin was followed by shelf and slope sedimentation in the Paleozoic. Preservation of basal Cambrian strata on different Belt units with angular unconformity 100 km to the north (Campbell, 1959; Lewis and others, 2002a) indicates that the Belt rocks were folded or faulted during one more of the Proterozoic deformational events (described above). No record exists within this map or adjacent areas of additional sedimentation or deformation in the Paleozoic or early Mesozoic.

The map covers a small part of the Rocky Mountain fold and thrust belt, which in turn is part of the Cordilleran fold and thrust belt of North America. Contraction during the Sevier orogeny migrated eastward as a result of plate convergence (e.g., Bird, 1998; DeCelles, 2004). Shortening across the belt exceeded 165 km in northwestern Montana (McMechan and Thompson, 1993). Gravity and seismic data across southern British Columbia, northern Idaho, and northwestern Montana are consistent with presence of crystalline basement above the basal décollement of the Rocky Mountain fold and thrust belt (Cook and van der Velden, 1995; Kleinkopf and others, 1997). Thus it seems plausible that most if not all pre-Cretaceous rocks exposed in the quadrangle are allochthonous, although some of the eastward transport may have been reversed by Eocene extension. If all rocks are allochthonous, the basal décollement is not exposed. The implication of this is that *Xqdg* and *Xan* and their country rock exist as slices of basement that are tectonically intermixed with overlying Proterozoic strata. This would explain proximity of Paleoproterozoic rocks with quartzite that contains younger detrital zircons. An alternative is that the basal décollement emerges over the anorthosite and its country rock that are autochthonous or parautocthonous. This is similar to the favored interpretation for the Archean Pend Oreille gneiss found low in the Spokane dome of the Priest River complex 130 km to the northwest (Doughty and others, 1998). In either alternative above, the younger quartzite could be basal to the Belt, or if the obscured contact is not a nonconformity, the younger quartzite could sit upon the Early Proterozoic rocks along an unrecognized detachment fault.

Thrust faulting may have started during the Sevier orogeny and before 100 Ma (Foster and others, 2001). House and others (1997) speculated that regional (M1) metamorphism was about 100-80 Ma and coincident with arc magmatism. Metamorphic zircon that formed at ~85-90 Ma in the *Ycs* unit (NF sample), is consistent with at least one metamorphic event at this time. Many Cretaceous magmas were emplaced at depth and those in the northwest part of the area were deformed into orthogneiss (*Kbtg, Kqdg*) during continuing contraction. Quartz diorite that intruded in the Headquarters area, at about 95 Ma, is less deformed. In the Bitterroot core complex to the southeast, peak metamorphism was coincident with 80-75 Ma syntectonic quartz diorite plutons although partial melting at lower and middle crustal depths continued to 65-53 Ma (Foster and others, 2001). M2 may have occurred during intrusion of similar age plutons of the Idaho batholith (Lang and Rice, 1985b). M1 and M2 isograds cross strata in the Packsaddle syncline to the north (Lang and Rice, 1985b), indicating that the syncline likely formed before M2 and was tilted up to the north afterwards. It is possible that large left-slip displacement on the Kelly Forks-Benton Creek fault system (Kell and Childs, 1999) and counter clockwise rotation of the Packsaddle syncline (Burmester and Lewis, 2003) were coincident with this tilting.

Intrusion of Eocene granite and granodiorite (*Tggd*) may have begun as early as 54 Ma, and continued until ~46 Ma. M3 is attributed to nonequlibrium rapid unroofing 56-48 Ma (Carey and others, 1992; Grover and others, 1992; House and others, 1997; Foster and others, 2001) and was probably synchronous with magmatic activity and regional extension. Eocene granite plutons such as the Bungalow (*Tg*) lack penetrative deformation. The chilled margins and miarolitic cavities in the *Tg* plutons are consistent with considerable uplift before, or during, this final phase of Eocene magmatism. Some extension likely was accommodated by intrusion of north-south striking dikes that are common near the Bungalow pluton. The apparent abrupt transition from high metamorphic grade rocks in and near the Boehls Butte anorthosite to lower(?) grade and little deformed Prichard Formation rocks south, east, and west suggests that regional uplift was facilitated by top-to-the-east extension and detachment faulting. Cooling of the rocks in the footwall of the Jug Rock mylonite zone did not occur until 47 Ma, based on $^{40}Ar/^{39}Ar$ cooling ages from muscovite (David Foster, written commun. to Doughty, 2004; Foster and others, in press). Right-lateral displacement on the Kelly Forks-Benton Creek fault system was coincident with this extension.

Columbia River basalts and related sediments covered the southwestern part of the area in the Miocene. Plant fossils in Miocene sediments show that the climate was warm and wet, similar to that of the southeast U.S. today (Smiley and Rember, 1979). Additionally, deep weathering, kaolinitic deposits, and paleosols that formed in Miocene sediments are relicts of the warm-climate chemical weathering, which may have continued into the Pliocene. The deep weathering produced saprolite that is common in the southwestern part of the map. Since the late Miocene, the major streams have cut canyons deep into the saprolitic surface and there have been landslides, primarily of basalt off of underlying sediment, into canyons. During the Pleistocene, alpine glaciers deposited till in valleys in the northern part of the map.

ACKNOWLEDGMENTS

Technical reviews by David Foster and Karen Lund of earlier versions of this map are greatly appreciated. Mapping and compilation were supported by the U.S. Geological Survey STATEMAP program, the U.S. Geological Survey office in Spokane, Washington, the Idaho Department of Lands, Potlatch Corporation, and an NSF grant (EAR 5-32280) awarded to P. Ted Doughty, Kevin Chamberlain, and Jim Sears. Doughty acknowledges the excellent field assistance and campfire discussions of Andy Buddington, Brian Boothe, and Rebecca Pitts. Grant Sha, who completed his M.S. at Washington State University on the Jug Rock fault zone, and John Watkinson, his major professor, are thanked for enthusiastic discussions.

REFERENCES

Abbott, A.T., and L.S. Prater, 1954, The geology of kyanite andalusite deposits, Goat Mountain, Idaho, and preliminary beneficiation tests on the ore: Idaho Bureau of Mines and Geology Pamphlet 100, 27 p.

Anderson, H.E., and D.W. Davis, 1995, U-Pb geochronology of the Moyie Sills, Purcell Supergroup, southeastern British Columbia: implications for the Mesoproterozoic geological history of the Purcell (Belt) Basin: Canadian Journal of Earth Sciences, v. 32, no. 8, p. 1180-1193.

Bird, P., 1998, Kinematic history of the Laramide orogeny in latitudes 35º-49º N, western United States: Tectonics, v. 17, p. 780-801.

Burmester, R.F., and R.S. Lewis, 2003, Counterclockwise rotation of the Packsaddle syncline is consistent with regional sinistral transpression across north-central Idaho: Northwest Geology, v. 23, p. 147-159.

Burmester, R.F., R.S. Lewis, and E.H. Bennett, 1998, Belt rocks north of the Bitterroot lobe of the Idaho batholith: the southwest basin margin, *in* R. B. Berg, ed., Belt Symposium III: Montana Bureau of Mines and Geology Special Publication 112, p. 145-156.

Burmester, R.F., W.C. McClelland, and R.S. Lewis, 2004, U-Pb dating of plutons along the transfer zone between the Bitterroot and Priest River metamorphic core complexes: Geological Society of America Abstracts with Programs, v. 36, no. 4, p. 72.

Camp, V.E., 1981, Geologic studies of the Columbia Plateau: Part II. Upper Miocene basalt distribution, reflecting source locations, tectonism, and drainage history in the Clearwater embayment, Idaho: Geological Society of America Bulletin, Part I, v. 92, p. 669-678.

Campbell, A.B., 1959, Precambrian-Cambrian unconformity in northwestern Montana and northern Idaho: Geological Society of America Bulletin, v. 70, no. 12, part 2, p. 1776.

Carey, J.W., J.M. Rice, and T.W. Grover, 1992, Petrology of aluminous schist in the Boehls Butte region of northern Idaho: Geologic history and aluminum-silicate phase relations: American Journal of Science, v. 292, p. 455-473.

Childs, J.F., 1982, Geology of the Precambrian Belt Supergroup and the northern margin of the Idaho batholith, Clearwater County, Idaho: Santa Cruz, University of California Ph.D. dissertation, 491 p.

Choiniere, S.R., and D.A. Swanson, 1979, Magnetostratigraphy and correlation of Miocene basalts of the northern Oregon coast and Columbia Plateau, southeast Washington: American Journal of Science, v. 279, p. 755-777.

Collins, B.W., 1999, The interstratal middle Wallace breccia: evidence of post-Wallace faulting: University of Montana B.A. senior thesis, 27 p.

Colpron, M., J.M. Logan, and J.K. Mortensen, 2002, U-Pb zircon age constraint for late Neoproterozoic rifting and initiation of the lower Paleozoic passive margin of western Laurentia: Canadian Journal of Earth Sciences, v. 9, no. 2, p. 133-143.

Cook, F.A., and A.J. van der Velden, 1995, Three-dimensional crustal structure of the Purcell anticlinorium in the Cordillera of southwestern Canada: Geological Society of America Bulletin, v. 107, p. 642-664.

Cressman, E.R., 1989, Reconnaissance stratigraphy of the Prichard Formation (Mesoproterozoic) and the early development of the Belt Basin, Washington, Idaho, and Montana: U.S. Geological Survey Professional Paper 1490, 80 p.

Day, Norm, 1975, Unpublished U.S. Forest Service map, Cedars Planning Unit, Clearwater National Forest.

DeCelles, P.G., 2004, Late Jurassic to Eocene evolution of the cordilleran thrust belt and foreland basin system, western U.S.A.: American Journal of Science, v. 304, p. 105-168.

Doughty, P.T., and A.M. Buddington, 2002, Eocene structural evolution of the Boehls Butte anorthosite and Clearwater core complex, north central Idaho: a basement-involved extensional strike-slip relay: Geological Society of America Abstracts with Programs, v. 34, no. 6, p. 332.

Doughty, P.T., and K.R. Chamberlain, 1996, The Salmon River arch revisited: new evidence for 1370 Ma rifting near the end of deposition in the Mesoproterozoic Belt basin: Canadian Journal of Earth Sciences, v. 86. p. 1037-1052.

Doughty, P.T., and K.R. Chamberlain, 2007, Age of Paleoproterozoic basement and related rocks in the Clearwater complex, northern Idaho, U.S.A., *in* P.K. Link and R.S. Lewis, eds., Proterozoic Geology of Western North America and Siberia: SEPM Special Publication. 86, p. 9-35.

Doughty, P.T., R.A. Price, and R.R. Parrish, 1998, Geology and U-Pb geochronology of Archean basement and Proterozoic cover in the Priest River complex, northwestern United States, and

their implications for Cordilleran structure and Precambrian continent reconstructions: Canadian Journal of Earth Science, v. 35, p. 39-54.
Doughty, P.T., and S.D. Sheriff, 1992, Paleomagnetic evidence for en echelon crustal extension and crustal rotations in western Montana and Idaho: Tectonics, v. 11, no. 3, p. 663-671.
Evans, K.V., J.N. Aleinikoff, J.D. Obradovich, and C.M. Fanning, 2000, SHRIMP U-Pb geochronology of volcanic rocks, Belt Supergroup, western Montana: evidence for rapid deposition of sedimentary strata: Canadian Journal of Earth Sciences, v. 37, no. 9, p. 1287-1300.
Evans, K.V., and L.B. Fischer, 1986, U-Pb geochronology of two augen gneiss terranes, Idaho B new data and tectonic implications: Canadian Journal of Earth Sciences, v. 23, p. 1919-1927.
Finch, J.C., and D.O. Baldwin, 1984, Stratigraphy of the Prichard Formation, Belt Supergroup, *in* S.W. Hobbs, ed., The Belt: Montana Bureau of Mines and Geology Special Publication 90, p. 5-7.
Foster, D.A., P.T. Doughty and T.J. Kalakay, in press, Exhumation and kinematics of metamorphic core complexes along the Lewis and Clark fault system: Geological Society of America Special Paper.
Foster, D.A., and C.M. Fanning, 1997; Geochronology of the northern Idaho batholith and the Bitterroot metamorphic core complex: Magmatism preceding and contemporaneous with extension: Geological Society of America Bulletin, v. 109, no. 4, p. 379-394.
Foster, D.A., T.J. Kalakay, P.T. Doughty, and C.M. Fanning, and J.J. Vogl, 2004, Kinematics of Eocene metamorphic core complexes in the northern Rocky Mountains: Geological Society of America Abstracts with Programs, v. 36, no. 4, p. 72.
Foster, D.A., Carl Schafer, C.M. Fanning, and D.W. Hyndman, 2001, Relationships between crustal partial melting, plutonism, orogeny, and exhumation: Idaho-Bitterroot batholith: Tectonophysics, v. 342, p. 313-350.
Freeman, W., and D. Winston, 1987, A quartz arenite blanket at the base of, or below the Mesoproterozoic Belt Supergroup? Montana and Idaho: Geological Society of America Abstracts with Programs, v. 19, no. 5, p. 276.
Garwood, D.L, 2001, Bedrock geology map of the Lewiston Orchards North and Lapwai 72-minute quadrangles, Nez Perce County, Idaho: University of Idaho M.S. thesis, 62 p.
Gaschnig, R.M., J. Vervoort, R.S. Lewis, E. King, and J. Valley, 2007, Multiple punctuated pulses of voluminous silicic magmatism in Idaho: in situ geochronology and isotope geochemistry of the Idaho batholith: Geological Society of America Abstracts with Programs, v. 39, no. 6, p. 608.
Goldberg, S.A., 1983, Geochemical constraints on the origin of Proterozoic anorthosites, western United States: University of Oregon Ph.D. dissertation, 191 p.
Grover, T.W., J.M. Rice, and J.W. Carey, 1992, Petrology of aluminous schist in the Boehls Butte region of northern Idaho: Phase equilibria and P-T evolution: American Journal of Science, v. 292, p. 474-507.
Heath, S.A, and H.W. Fairbairn, 1969, Sr^{87}/Sr^{86} ratios in anorthosites and some associated rocks, *in* Y.W. Isachsen, ed., Origin of Anorthosite and Related Rocks: New York State Museum and Science Service Memoir 18, p. 99-110.
Hietanen, Anna, 1962, Metasomatic metamorphism in western Clearwater County Idaho: U.S. Geological Survey Professional Paper 344-A, 113 p., scale 1:48,000.
Hietanen, Anna, 1963a, Anorthosite and associated rocks in the Boehls Butte quadrangle and vicinity, Idaho: U.S. Geological Survey Professional Paper 344-B, 78 p., scale 1:48,000.
Hietanen, Anna, 1963b, Idaho batholith near Pierce and Bungalow, Clearwater County, Idaho: U.S. Geological Survey Professional Paper 344-D, 42 p., scale 1:48,000.
Hietanen, Anna, 1968, Belt series in the region around Snow Peak and Mallard Peak, Idaho: U.S. Geological Survey Professional Paper 344-E, 34 p., scale 1:48,000.
Hietanen, Anna, 1969, Metamorphic environment of anorthosite in the Boehls Butte area, Idaho, *in* Isachsen, Y.W., ed., The origin of anorthosite and related rocks: New York State Museum and Science Memoir 18, p. 371-386.
Hietanen, Anna, 1984, Geology along the northwest border zone of the Idaho batholith: U.S. Geological Survey Bulletin 1608, 16 p.
Hooper, P.R., 2000, Chemical discrimination of Columbia River basalt flows: Geochemistry Geophysics Geosystems (G3), v. 1, June 12, 2000, paper no. 2000GC000040.

House, M.A., K.V. Hodges, and S.A. Bowring, 1997, Petrological and geochronological constraints on regional metamorphism along the northern border of the Bitterroot batholith: Journal of Metamorphic Geology, v. 15, no. 6, p. 753-764.

Höy, T., 1993, Geology of the Purcell Supergroup in the Fernie West-Half map area, southeastern British Columbia: British Columbia Ministry of Energy, Mines and Petroleum Resources, Bulletin 84, 110 p.

Huebschman, R.P., 1973, Correlation of fine carbonaceous bands across a Precambrian stagnant basin: Journal of Sedimentary Petrology, v. 43, p. 688-699.

Hutchison, C.S., 1981, Belt orogenesis along the northern margin of the Idaho batholith: Idaho Bureau of Mines and Geology Technical Report 81-2, 54 p.

Juras, D.S., 1974, The petrofabric analysis and plagioclase petrography of the Boehl's Butte anorthosite: University of Idaho Ph.D. dissertation, 132 p.

Kauffman, J.D., 2004a, Geologic map of the Gifford quadrangle, Nez Perce County, Idaho: Idaho Geological Survey Geologic Map 36, scale 1:24,000.

Kauffman, J.D., 2004b, Major oxide and trace element analyses for volcanic rocks in northern Idaho, 1978-2002: Idaho Geological Survey Digital Analytical Data 1, excel spreadsheet.

Kell, R.E., and J.F. Childs, 1999, Mesozoic-Cenozoic structural events affecting the Belt Basin between the Idaho batholith and the Lewis and Clark line: implications on identifying syndepositional Belt-age structures, *in* R.B. Berg, ed. Belt Symposium III Abstracts, 1993: Montana Bureau of Mines and Geology Open-File Report 381, p. 32-34.

Kleinkopf, M.D., J.E. Harrison, and W.D. Stanley, 1997, Geophysical interpretations of the Libby thrust belt, northwestern Montana: U.S. Geological Survey Professional Paper 1546, 22 p.

Lang, H.M., and J.M. Rice, 1985a, Geothermometry, geobarometry and T-X(Fe-Mg) relations in metapelites, Snow Peak, northern Idaho: Journal of Petrology, v. 26, no. 4, p. 889-924.

Lang, H.M., and J.M. Rice, 1985b, Metamorphism of pelitic rocks in the Snow Peak area, northern Idaho: sequence of events and regional implications: Geological Society of America Bulletin, v. 96, no. 6, p. 731-736.

Larson, P.B., and Z.D. Sharp, 1998, Mineral oxygen isotope ratios for the Boehls Butte-Goat Mountain metamorphic complex, Idaho: Evidence for fast cooling: American Journal of Science, v. 298, no. 7, p. 572-593.

Leach, G.B., 1962, Metamorphism and granitic intrusion of Precambrian age in southeastern British Columbia: Geological Survey of Canada., Paper 62-13, 8 p.

Lemoine, S.R., and Don Winston, 1986, Correlation of the Snowslip and Shepard formations of the Cabinet Mountains with upper Wallace rocks of the Coeur d'Alene Mountains, western Montana, *in* S.M. Roberts, ed., Belt Supergroup: A Guide to Proterozoic Rocks of Western Montana and Adjacent Areas: Montana Bureau of Mines and Geology Special Publication 94, p. 161-168.

Lewis, R.S., R.F. Burmester, and E.H. Bennett, 1998, Metasedimentary rocks between the Bitterroot and Atlanta lobes of the Idaho batholith and their relationship to the Belt Supergroup, *in* R.B. Berg, ed., Belt Symposium III: Montana Bureau of Mines and Geology Special Publication 112, p. 130-144.

Lewis, R.S., R.F. Burmester, M.D. McFaddan, B.A. Eversmeyer, C.A. Wallace, and E.H. Bennett, 1992a, Geologic map of the upper North Fork of the Clearwater River drainage, northern Idaho: Idaho Geological Survey Geologic Map 20, scale 1:100,000.

Lewis, R.S., R.F. Burmester, R.W. Reynolds, E.H. Bennett, P.E. Myers, and R.R. Reid, 1992b, Geologic map of the Lochsa River area, northern Idaho: Idaho Geological Survey Geological Map 19, scale 1:100,000.

Lewis, R.S., R.F. Burmester, M.D. McFaddan, P.D. Derkey, and J.R. Oblad, 1999, Digital geologic map of the Wallace 1:100,000 quadrangle, Idaho: U.S. Geological Survey Open-File Report 99-390.

Lewis, R.S., R.F. Burmester, J.D. Kauffman, and T.P. Frost, 2000, Geologic map of the St. Maries 30' x 60' quadrangle, Idaho: Idaho Geologic Survey Geologic Map 28, scale 1:100,000.

Lewis, R.S., R.F. Burmester, R.M Breckenridge, M.D. McFaddan, and J.D. Kauffman, 2002a, Geologic map of the Coeur d'Alene 30' x 60' quadrangle, Idaho: Idaho Geologic Survey Geologic Map 33, scale 1:100,000.

Lewis, R.S., J. H. Bush, R.F. Burmester, J.D. Kauffman, D.L. Garwood, P.E. Myers, and K.L. Othberg, 2005, Geologic map of the Potlatch 30' x 60' quadrangle, Idaho: Idaho Geological Survey Geologic Map 41, scale 1:100,000.

Lewis, R.S., and T.P. Frost, 2005, Major oxide and trace element analyses for igneous and metamorphic rock samples from northern and central Idaho: Idaho Geological Survey Digital Analytical Data 2.

Lewis, R.S., R.F. Burmester, T.P. Frost, and W.C. McClelland, 2002b, Newly mapped Eocene strike-slip faults south of the Boehls Butte anorthosite, northern Idaho: Geological Society of America Abstracts with Programs, v. 34, no. 5, p. 84.

Lewis, R.S., J.D. Vervoort, R.F. Burmester, W.C. McClelland, and Zhaoshan Chang, 2007, Geochronological constraints on Mesoproterozoic and Neoproterozoic(?) high-grade metasedimentary rocks of north-central Idaho, *in* P.K. Link and R.S. Lewis, eds., Proterozoic Geology of Western North America and Siberia: SEPM Special Publication 86, p. 37-53.

Lund, Karen, J.N. Aleinikoff, K.V. Evans, and C.M. Fanning, 2003, SHRIMP U-Pb geochronology of Neoproterozoic Windermere Supergroup, central Idaho: implications for rifting of western Laurentia and synchroneity of Sturtian glacial deposits: Geological Society of America Bulletin, v. 115, no. 3, p. 349-372.

McFarlane, C.R.M., and D.R.M. Pattison, 2000, Geology of the Matthew Creek metamorphic zone, southeast British Columbia: a window into Mesoproterozoic metamorphism in the Purcell Basin: Canadian Journal Earth Sciences, v. 37, p. 1073-1092.

McKee, E.H., D.A. Swanson, and T.L. Wright, 1977, Duration and volume of Columbia River Basalt volcanism, Washington, Oregon, and Idaho: Geological Society of America Abstracts with Programs, v. 9, no. 4, p. 463-464.

McMechan, M.E., and R.A. Price, 1982, Superimposed low-grade metamorphism in the Mount Fisher area, southeastern British Columbia: implications for the East Kootenay Orogeny: Canadian Journal of Earth Sciences, v. 19, p. 476-489.

McMechan, M.E., and R.I. Thompson, 1993, The Canadian Cordilleran fold and thrust belt south of 66 degrees N and its influence on the Western Interior Basin, *in* W.G.E. Caldwell and E.G. Kauffman, eds., Evolution of the Western Interior Basin: Geological Association of Canada Special Paper 39, p. 73-90.

Miller, F.K., 1994, The Windermere Group and late Proterozoic tectonics in northeastern Washington and northern Idaho, *in* Raymond Lasmanis and E.S. Cheney, Regional Geology of Washington State: Washington Department of Natural Resources, Division of Geology and Earth Resources, Bulletin 80, p. 1-19.

Mora, C.I, and K. Ramseyer, 1992, Cathodoluminescence of coexisting plagioclases, Boehls Butte anorthosite; CL activators and fluid flow paths: American Mineralogist, v. 77, no. 11-12, p. 1258-1265.

Mora, C.I., L.R. Riciputi, and D.R. Cole, 1999, Short-lived oxygen diffusion during hot, deep-seated meteoric alteration of anorthosite: Science, v. 286, no. 5448, p. 2323-2325.

Mueller, P., D. Foster, J. Wooden, D. Mogk, and R. Lewis, 2003, Archean and Proterozoic sources for basal quartzites from the eastern and western margins of the Belt basin: Northwest Geology, v. 32, p. 215-216.

Nord, G.L., Jr., 1973, The origin of the Boehl's Butte anorthosite and related rocks, Shoshone County, Idaho: Berkeley, University of California Ph.D. dissertation, 159 p.

Reid, R.R., D.A. Morrison, and W.R. Greenwood, 1973, The Clearwater orogenic zone: A relict of Proterozoic orogeny in central and northern Idaho: Idaho Bureau of Mines and Geology, Belt Symposium I, vol. 1, p. 10-56.

Reidel, S.P., and K.R. Fecht, 1987, The Huntzinger flow: evidence of surface mixing of the Columbia River Basalt and its petrogenetic implications: Geological Society of America Bulletin 98, p. 664-677.

Rietman, J.D., 1966, Remanent magnetization of the late Yakima Basalt, Washington State: Stanford University Ph.D. dissertation, 87 p.

Reynolds, R.W., 1991, Petrology and geochemistry of the Bungalow pluton and associated hypabyssal dikes, Clearwater County, Idaho: University of Idaho M.S. thesis, 204 p.

Ross, G.M., and M. Villeneuve, 2003, Provenance of the Mesoproterozoic (1.45 Ga) Belt basin (western North America): another piece in the pre-Rodinia paleogeographic puzzle: Geological Society of America Bulletin, v. 115, p. 1191-1217.

Ruendal, A.P., 1987, Petrology of sillimanite-grade metapelites in the Headquarters area, northern Idaho: University of Oregon M.S. thesis, 111 p.

St. Godard, E.N.J., 1998, Sediment dispersal pathways in quartzite units of the Lower Prichard Formation, Pine Creek drainage, Idaho, *in* R.B. Berg, ed., Belt Symposium III: Montana Bureau of Mines and Geology Special Publication 112, p. 44-55.

Sears, J.W., K.R. Chamberlain, and S.N. Buckley, 1998, Structural and U-Pb geochronological evidence for 1.47 Ga rifting in the Belt basin, western Montana: Canadian Journal of Earth Science, v. 35, p. 467-475.

Seyfert, C.K., 1984, The Clearwater Core Complex, a new Cordilleran metamorphic core complex, and its relation to a major continental transform fault: Geological Society of America Abstracts with Programs, v. 16, no. 6, p. 651.

Sha, G.S., 2004, The tectonic evolution of the Boehls Butte-Clearwater core complex, north-central Idaho: Washington State University M.S. thesis, 143 p.

Sha, G.S., J.D. Vervoort, A.J. Watkinson, P.T. Doughty, Julie Prytulak, R.G. Lee, and P.B. Larson, 2004, Geochronologic constraints on the tectonic evolution of the Boehls Butte-Clearwater core complex: evidence from 1.01 Ga garnets: Geological Society of America Abstracts with Programs, v. 36, no. 4, p. 72.

Smiley, C.J. and W.C. Rember, 1979, Guidebook and road log to the St. Maries River (Clarkia) fossil area of northern Idaho: Idaho Geological Survey Information Circular 33, 27 p.

Standish, R.P., 1973, Structural geology and metamorphism of the Mallard-Larkins Peak area, Clearwater and Shoshone counties, Idaho: University of Idaho M.S. thesis, 82 p.

Streckeisen, A.L., 1976, To each plutonic rock its proper name: Earth-Science Reviews, v. 12, p. 1-33.

Stryhas, B.A., 1985a, Structural analysis of Five Lakes Butte, northeast Idaho: University of Idaho M.S. thesis, 93 p.

Stryhas, B.A., 1985b, Geologic map of Five Lakes Butte, Shoshone County, Idaho: Idaho Geological Survey Technical Report 85-11, scale 1:3,600.

Swanson, D.A., J.E. Anderson, R.D. Bentley, G.R. Byerly, V.E. Camp, J.N. Gardner, and T.L. Wright, 1979a, Reconnaissance geologic map of the Columbia River Basalt Group in eastern Washington and northern Idaho, Pullman 1° x 2° quadrangle: U.S. Geological Survey Open-File Report 79-1363, sheet 8 of 12, scale 1:250,000.

Swanson, D.A., T.L. Wright, P.R. Hooper, and R.D. Bentley, 1979b, Revisions in stratigraphic nomenclature of the Columbia River Basalt Group: U.S. Geological Survey Bulletin 1457-G, 59 p.

Toth, M.I., and J.S. Stacey, 1992, Constraints on the formation of the Bitterroot lobe of the Idaho batholith, Idaho and Montana, from U-Pb zircon geochronology and feldspar Pb isotopic data: U.S. Geological Survey Bulletin 2008, 14 p.

Vervoort, J.D., W.C. McClelland, J.S. Oldow, , A.J. Watkinson, and G. Sha, 2005, Grenville-age metamorphism on the western margin of Laurentia, northern Idaho; evidence from Lu-Hf garnet geochronology: Geological Society of America Abstracts with Programs, v. 37, no. 7, p. 89.

Vervoort, J.D., N.A. Zirakparvar, R.S. Lewis, R.S., and R.F. Burmester, 2007, Evidence for recurrent Paleoproterozoic and Mesoproterozoic magmatism and metamorphism in the Boehls Butte-Clarkia area, north-central Idaho, U.S.A.: Geological Society of America Abstracts with Programs, v. 39, no. 6, p. 245.

Walker, K.D., 1993, Mineralogy and oxygen isotope composition of the Boehls Butte anorthosite, northern Idaho: University of Tennessee M.S. thesis, 111 p.

Wentworth, C.K., 1922, A scale of grade class terms for clastic sediments: Journal of Geology, v. 30, no. 5, p. 377-392.

White, W.H., 1959, Cordilleran tectonics in British Columbia: American Association of Petroleum Geologists Bulletin, v. 43, p. 60-100.

Zieg, G.A., 1986, Stratigraphy and sedimentology of the Mesoproterozoic upper Newland Limestone, *in* S.M. Roberts, ed., Belt Supergroup: A Guide to Proterozoic Rocks of Western Montana and Adjacent Areas: Montana Bureau of Mines and Geology Special Publication 94, p. 125-142.

Ziegler, R.D., 1991, Petrology of garnet amphibolites from the Boehls Butte quadrangle, northern Idaho: University of Oregon M.S. thesis, 116 p.